

Review

Recent Developments in Plasmonic Sensors of Phenol and Its Derivatives

Nguyễn Hoàng Ly ¹, Sang Jun Son ¹, Ho Hyun Kim ^{2,*} and Sang-Woo Joo ^{3,*}

¹ Department of Chemistry, Gachon University, Seongnam 13120, Korea; nguyenhoangly2007@gmail.com (N.H.L.); sjson@gachon.ac.kr (S.J.S.)

² Department of Integrated Environmental Systems, Pyeongtaek University, Pyeongtaek 17869, Korea

³ Department of Chemistry, Soongsil University, Seoul 06978, Korea

* Correspondence: ho4sh@ptu.ac.kr (H.H.K.); sjoo@ssu.ac.kr (S.-W.J.)

Abstract: Many scientists are increasingly interested in on-site detection methods of phenol and its derivatives because these substances have been universally used as a significant raw material in the industrial manufacturing of various chemicals of antimicrobials, anti-inflammatory drugs, antioxidants, and so on. The contamination of phenolic compounds in the natural environment is a toxic response that induces harsh impacts on plants, animals, and human health. This mini-review updates recent developments and trends of novel plasmonic resonance nanomaterials, which are assisted by various optical sensors, including colorimetric, fluorescence, localized surface plasmon resonance (LSPR), and plasmon-enhanced Raman spectroscopy. These advanced and powerful analytical tools exhibit potential application for ultrahigh sensitivity, selectivity, and rapid detection of phenol and its derivatives. In this report, we mainly emphasize the recent progress and novel trends in the optical sensors of phenolic compounds. The applications of Raman technologies based on pure noble metals, hybrid nanomaterials, and metal–organic frameworks (MOFs) are presented, in which the remaining establishments and challenges are discussed and summarized to inspire the future improvement of scientific optical sensors into easy-to-operate effective platforms for the rapid and trace detection of phenol and its derivatives.

Keywords: phenolic compounds; plasmonic resonance; Raman spectroscopy; noble metal nanostructures; environmental detection



Citation: Ly, N.H.; Son, S.J.; Kim, H.H.; Joo, S.-W. Recent Developments in Plasmonic Sensors of Phenol and Its Derivatives. *Appl. Sci.* **2021**, *11*, 10519. <https://doi.org/10.3390/app112210519>

Academic Editor: Francisco Pérez-Ocón

Received: 29 September 2021

Accepted: 3 November 2021

Published: 9 November 2021

Publisher's Note: MDPI stays neutral with regard to jurisdictional claims in published maps and institutional affiliations.



Copyright: © 2021 by the authors. Licensee MDPI, Basel, Switzerland. This article is an open access article distributed under the terms and conditions of the Creative Commons Attribution (CC BY) license (<https://creativecommons.org/licenses/by/4.0/>).

1. Introduction

Plasmonic resonance-based optical sensor technology has been considered to be an efficient method applied for sensing techniques of either indoor or outdoor carbon dioxide molecules [1], various gases [2], inorganic arsenic compounds [3], and pesticides [4]. Optical sensors have been known as simple analytical techniques to demonstrate numerous advantages such as facile design and effective detection, leading to promising potential applications in environmental metal ion monitoring [5]. Recently, plasmonic nanomaterials [6] and 2D materials [7] have rapidly emerged as unique sensing platforms for varieties of engineering applications thanks to their specific features such as enhanced electrical, optical, and electrochemical signals.

Among various optical sensor materials, scientists are increasingly interested in pure noble metals and combined structures of hybrids and MOFs to utilize their plasmonic resonance. For example, some scientific reports have been published, such as an SPR sensor of Hg²⁺ [8], Au-modified-tyrosinase enzyme-based graphene oxide used for phenol detection [9], dopamine-inspired Au-assisted Raman monitoring of Cd²⁺ and polycyclic aromatic hydrocarbons [10], Au@Ag nanorod dimer-introduced dopamine detection [11], Ag nanocube-assisted Raman detection of protein [12] and thiram [13], and Ag-coated Au nanostar-supported Raman sensing of microplastic pollutants in water [14].

Phenol—also called benzenol, or mono-hydroxybenzene—has been known as the simplest compound of the aromatic alcohol group. Its main structure includes a benzene ring and a hydroxyl group (—OH) binding directly to one C atom of the aromatic ring. Although phenol can be toxic and its solutions with high concentration induce burned skin, it has been widely used as either primal raw materials or significant intermediates for the modern industrial manufacturing of many household products. For example, phenol with a suitable concentration has been used as one of the important ingredients in a mouth rinse thanks to its efficient bactericidal features. In industrial products, phenol has been widely adapted to use as an indispensable material to manufacture synthetic textiles, phenolic resins, plastics, dyes, and aspirin. Besides the benefits, phenols also caused serious chemical accidents through leakage [15], attracting many concerns of environmental scientists and governments owing to its negative risk impact on humans and the environment. For example, some researchers have recently investigated the ecotoxicity of phenol on four marine microalgae [16], the toxicological effects of phenol and cresols on aquatic organisms [17], and deriving hazardous concentrations of phenol in soil ecosystems [18].

Recently, various optical sensor techniques have been developed, such as colorimetric [19,20], fluorescence [21,22], LSPR phenomenon [23,24], and plasmon-enhanced surface enhanced Raman scattering (SERS) [25–27]. Among these techniques, the SERS method based on plasmonic resonance nanomaterials is promising because of its high specific, selective, and sensitive detection capability. Combining nanostructured materials, as an effective plasmonic resonance phenomenon, with Raman spectroscopy is becoming a potential analytic tool for trace detection of analyte molecules with many advantages such as easy-to-use, low-cost, specific targets, and on-site detection. Specific studies on the development of several novel nanomaterials have been reported to assist effective Raman platforms including nanogold film-based Raman detection of rhodamine 6G and *p*-nitrophenol [28], Raman detection of multiple analytes based on Ag nanoparticle-modified SiO₂ nanofibrous [29], Ag nanostructure-assisted Raman sensing for monofluoroacetic acid [30], Ag nanoparticle-introduced Raman detection of carbofuran [31], on-site Raman detection of 1,2,3-benzotriazole on colloidal lignin particles [32], Ag-capped silicon nanopillar-based Raman detection of ochratoxin A [33], nano-shell composite array-based Raman sensor for antioxidant [34], and bimetallic plasmonic nanoparticle-assisted Raman detection of hazardous contamination [35]. Moreover, a series of scientific reports on several special metal–organic framework (MOF) structures has been investigated, leading to successful fabrication of novel Raman substrates applied in trace detection of phenol red [36], phenol-soluble modulin [37], and engine oil [38].

Phenolic compounds—such as catechol, *p*-nitrophenol, 2,4-dichlorophenol, 2,6-dichlorophenol (2,6-DCP), cresol, 4-*tert*-butylphenol, 4-*tert*-octylphenol, alpha-naphthol, dopamine, and so on—have been listed as hazardous substances by the United States Environmental Protection Agency owing to their toxicity [39]. Besides their significant potential application in industrial manufacturing, these compounds still faced some issues including environmental pollution and harmful effects on human health, in their included chemical products such as antioxidants, antimicrobials, and anti-inflammatory reagents that have been widely used in the daily activities of people [40,41].

In addition, 2,6-DCP—one of the most significant chlorophenol compounds—has been widely applied in industrial manufacturing for several chemicals, medical compounds, and other products, despite being potentially carcinogenic [42]. Recently, organic compounds with high toxicity such as *p*-nitrophenol have been found to cause increasingly serious pollution in environmental water [28]. As bisphenol substances have been considered as having a serious impact on the environment and human health risks, the early monitoring of these compounds is not only significant, but also still has many challenges.

Recently, there have been a large number of scientific reviews promising not only therapeutic applications of phenolic acids [43,44], but also phenolic compound's effects on the environment and human health risk [25,45]. Furthermore, several authors have investigated varieties of analytical technologies using trace detection of phenolic sub-

stances such as electrochemical [39,46–49], liquid chromatography with diode array and mass spectrometry [50], high performance liquid chromatography [51,52], conductometric biosensor [53], photoelectrochemical reduction [54], voltammetric detection [55,56], biosensor electrode [57], and nanomaterial-based sensing [58]. However, these methodologies often require additional procedures for separation of analytes in sample preparation, leading to time-consuming and toxic organic solvents, as well as adverse effects on the environment. Detection of phenols still needs more consideration, focusing on the novel detection methods such as plasmonic resonance-based optical sensors.

Plasmonic resonance phenomenon-based Raman sensing has emerged as a scientific tool for detecting analytes using molecular vibrations on nanomaterial surfaces [59]. Raman technology has related to LSPR in terms of introducing nanogap-enhanced plasmonic behaviors on noble metal surfaces [60]. Raman scattering as a supplementary application in which LSPR plays a significant role, has been introduced to pollutant monitoring [61]. Although there have been several reports on surface plasmon-based Raman sensors for detecting phenolic substances [59–61], there is no literature review, despite their universal application. We evaluate and discuss the recent development and trends in designing unique structured materials that aid in plasmonic sensor platforms used for efficient detection of phenolic substances that affect the human health risk in this review to understand the correlations between the Raman technique and plasmonic resonance phenomena (Figure 1). The main content used for on-site detection of phenolic compounds using plasmonic resonance-based optical sensors can be divided into four parts: (1) colorimetric, (2) fluorescence, (3) localized SPR, and (4) Raman detection based on sensing platforms of pure noble metals, hybrid nanomaterials, and MOF structures.

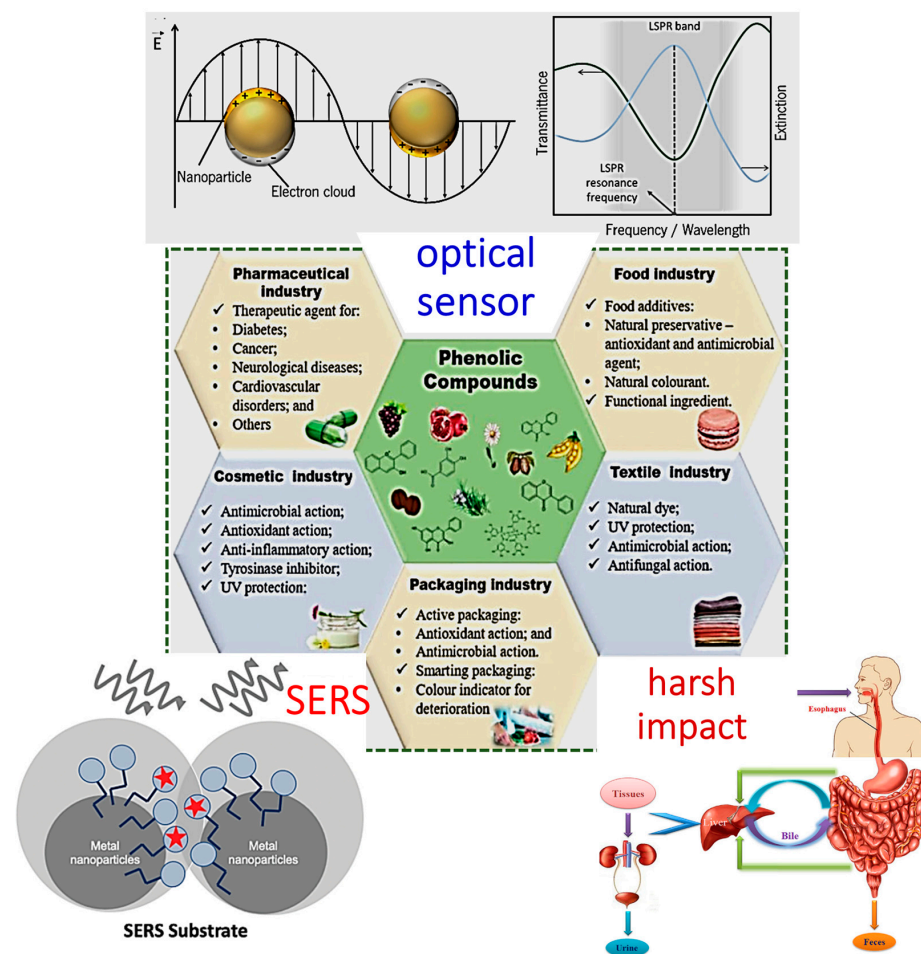


Figure 1. Applications of plasmonic resonance-based optical sensor for on-site detection of phenolic compounds that impact the human health risk. Adapted from [2,31,43,44] with permission.

2. Plasmonic Resonance-Based Colorimetric Sensor for Phenolic Compounds

The colorimetric sensor is a simple method that has been widely used in the selective detection of analytes using color changes in probes under unique conditions. This method can be widely applied in environmental gas sensing [62] and trace detection of tetracyclines in foods [63] thanks to its convenient performance. For example, a paper-based bioassay has been developed by assembling alginate and chitosan layer-by-layer. A tyrosinase enzyme has been used to bind these layers, leading to successful bioassay-based colorimetric sensing of not only phenol, but also bisphenol A, catechol, and cresols. The detection limit of these phenolic substances has been estimated at $0.86 (\pm 0.1) \mu\text{g/L}$ for each of the analytes [64]. A colorimetric sensor, based on plasmonic resonance nanomaterials, is one of the best analytical techniques for the efficient detection of various phenolic compounds by observing the color change of nanomaterials with either UV/Vis or the naked eye [39]. The basic principle of colorimetric technology is based on the specific interaction between the analytes with either pristine or probe-modified nanomaterials. For illustration, single-stranded DNA-regulated gold nanoparticle (GNP)-based colorimetric sensors have been demonstrated as an effective indicator for the sensitive detection of phenols [65]. As shown in Figure 2A, colorimetric detection of phenol has been successfully performed using Fenton reaction with a mixture of single-stranded DNA and initial GNPs. The authors have found that single-stranded DNA assisted in making initial GNPs more stabilized owing to electrostatic repulsion, leading to the prevention of GNP aggregation under the NaCl-introduced condition. However, these single-stranded DNAs have been destroyed by the Fenton reagents (OH free-radical) generating small fragments as mono- or oligonucleotide, resulting in the disruption of AuNP stability. In the presence of the phenolic substances, a reduction–oxidation between Fenton reagents and phenolic compounds will firstly occur to avoid the destruction of single-stranded DNA to assist the stability of GNPs from NaCl-induced aggregation. Meanwhile, Figure 2B illustrates that OH free-radical generated from Fenton reagents could attack catechol, leading to a reduction in phenolic compounds. Either with the naked eye or using UV/Vis spectroscopy, a GNP-assisted sensor exhibits rapid micromolar detection of catechol and hydroquinone.

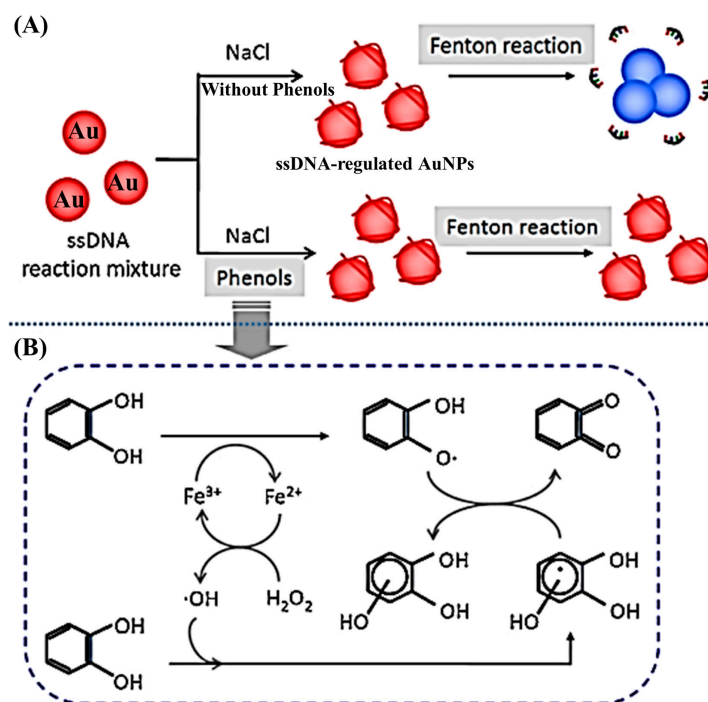


Figure 2. (A) AuNP-based colorimetric sensor for phenols' detection by means of Fenton reaction. (B) Schematic diagram of the mechanism of catechol oxidation owing to OH free-radicals generated from Fenton reagents. Adapted from [65].

Colorimetric detection of bisphenol A has been successfully performed using specific aptamer-based and cationic polymer-assisted GNP aggregation with a limited detection as low as 1.50 nM [66]. In contrast, an aptasensor-based and GNP-assisted colorimetric technique has been developed for ultra-sensitive detection of bisphenol A. In this study, the authors have reported that GNPs have been modified with the two types of specific aptamers as truncated 38-mer and 12-mer, leading to the limits of bisphenol A detection of 7.60 pM and 14.41 pM, respectively [67]. On the other hand, elliptical or sphere shapes of Fe₃O₄ nanoparticles with an average size of 7 nm indicate successful colorimetric detection of phenol in a range of 1–200 mM concentration [19]. Among various plasmon resonance nanomaterials, spherical Au nanostructures are well-known as the best colorimetric sensing units. Recently, special MOF structures have emerged as a novel material construction successfully applied in colorimetric detection. Numerous MOF structures with tunable colorimetric characteristics have been well designed and synthesized, aiming to be applied for sensing various analytes, including organic compounds and gaseous pollutants [68].

Furthermore, some specific studies on smart MOF nanomaterials can effectively detect contaminants of phenolic compounds in the environment, which are extremely significant for human health protection. For example, the dual-functional Co-MOF-74-based Co₃O₄ nanoparticle-decorated cellulose derivative membrane has been well-synthesized for colorimetric detection of phenol [69]. Moreover, Zr-based MOFs capped with polyvinylpyrrolidone have been reported to successfully contribute to the application of colorimetric detection of phenol [70]. However, relying on the self-assembly of copper ions and DNA, the authors have successfully fabricated a novel copper hybrid nanoflower, which induces a new paper-based microfluidic device. This device has displayed effective application for the colorimetric detection of catechol, dopamine, and hydroquinone [20]. In addition, UV/Vis detection of 2,4-dichlorophenol has been successfully performed using an enzyme mimic that has been well-synthesized by Cu ion and adenosine monophosphate [71].

Through a solvothermal route, a new core-shell nanostructured metal of Au and Ni (Au@Ni) with a size < 8 nm on reduced graphene oxides (rGOs) was designed to obtain a novel nanomaterial composite as Au@Ni/rGO (Figure 3A). Subsequently, the peroxidase mimetic feature of this nanocomposite was checked by analyzing the process oxidation of 3,3',5,5'-tetramethylbenzidine in H₂O₂. As shown in Figure 3B, the examined results indicated that this nanocomposite exhibited excellent peroxidase mimetic activity, which has been successfully applied in colorimetric detection of phenol, relying on its oxidative reaction with 4-aminoantipyrine, thereby inducing a change from colorless to pink of the quinoid dye in the presence of H₂O₂. The detection limit and range of this method have been estimated for phenol concentrations as low as 1.68 μM and 1–300 μM, respectively. In addition, under natural irradiated sunlight, these Au@Ni/rGO nanostructures exhibit an excellent photocatalytic reaction, thereby degrading over 87% of phenol and phenolic substances as 2-chlorophenol and 2-nitrophenol [72]. However, reduced graphene-based magnetic MOF nanocomposites exhibited an excellent enzyme-like feature. Phenol can be identified based on this property using a visual colorimetric method in water solution by oxidization of 4-aminoantipyrine in the presence of H₂O₂. Simultaneously, these nanocomposites have also been exposed to a specific feature as a Fenton-like catalyst, which shows a high ability to degrade phenol effectively [73].

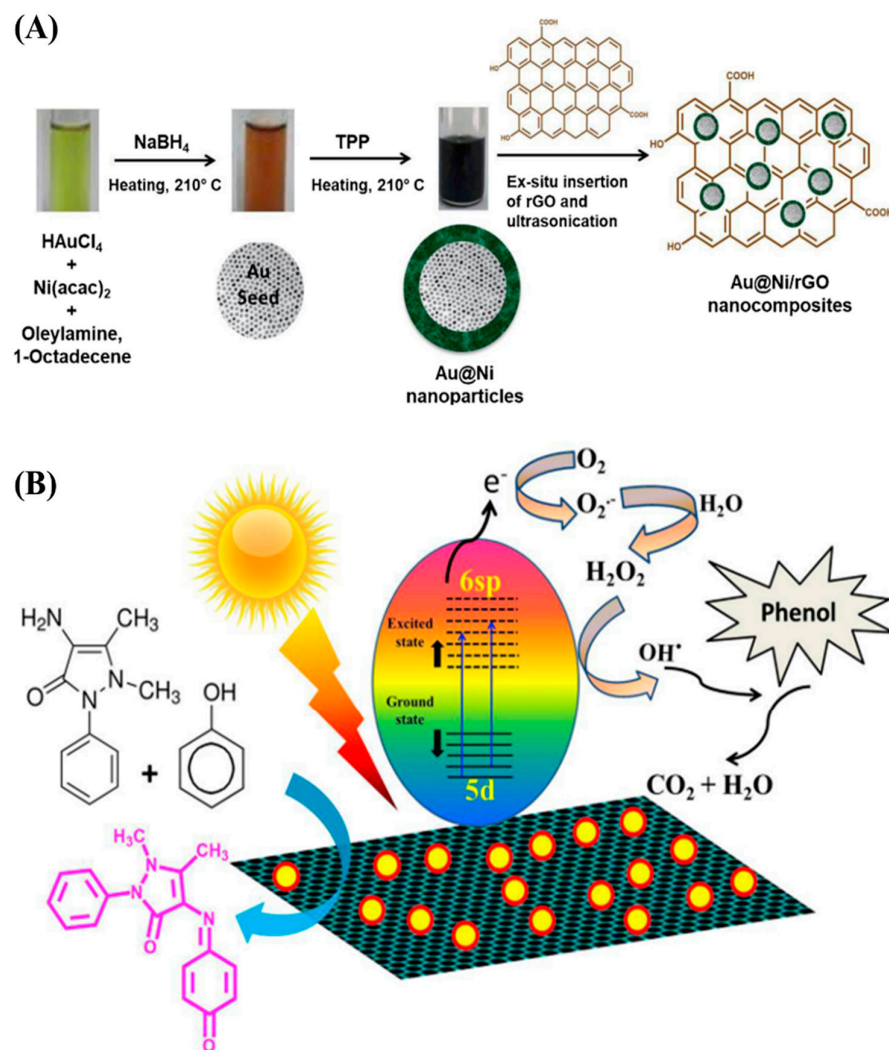


Figure 3. (A) Schematic diagram of Au@Ni/rGO-based colorimetric detection and degradation of phenol. (B) Schematic diagram of mechanism of core-shell nanocomposite-assisted colorimetric detection of phenol. Adapted from [72].

3. Plasmonic Resonance-Based Fluorescence Sensor for Phenolic Compounds

As a normal type of optical sensor, fluorescence techniques have been extensively applied in many fields, such as fast detection of phenolic substances [22], bioimaging [74], detection of aniline [75], determination of peroxyxynitrite products [76], analysis of total phenolic substances in teas [21], quantification of bisphenol A and its derivatives [77], determination of phenolics [78], and aptamer-labeled fluorescent detection of bisphenol A [79]. Plasmonic resonance-based fluorescence method has been used predominantly, because of its excellent plasmonic resonance mechanism. Various scientific studies have reported the successful fabrication of novel plasmonic resonance nanomaterials that exhibit uniform geometries and enhanced plasmon, aiming to assist fluorescence technology. Great efforts have been made on new nanomaterials with high plasmon resonance, such as AgNP-based fluorescence sensors for trace detection of dopamine [80], bimetallic Au-Ag nanocluster-assisted fluorescent biosensing of dicofol [81], polyethyleneimine-modified ovalbumin-stabilized gold nanoclusters (AuNCs) used for fluorescence sensor of tetracyclines [82], and MOF-based fluorescence detection of bisphenol substances [40]. A fluorescent sensor of 2,6-dimethyl phenol in seawater has been successfully performed relying on Eu^{3+} -2-aminoterephthalate immobilized on mesoporous silica nanoparticles [83].

As shown in Figure 4, although dopamine has been known as one of the most significant neurotransmitters in the human body, its specific monitoring remains many chal-

lenging. Using a one-pot process, the authors successfully fabricated bimetallic Au-Ag nanoclusters using a protein template as bovine serum albumin. These initial Au-Ag hybrid nanoclusters have been found to exhibit a weak level of fluorescent intensity. However, dopamine has been introduced to enhance the extremely strong fluorescent intensity of nanoclusters, simultaneously causing a red shift in the spectrum. Using electrochemical spectroscopy, dopamine has contributed to reducing Au-Ag hybrid nanoclusters, enhancing their fluorescence, which has been adopted for trace and sensitive detection of dopamine. This facile and efficient method provided a limit of detection of dopamine at 6.9 nM [84].

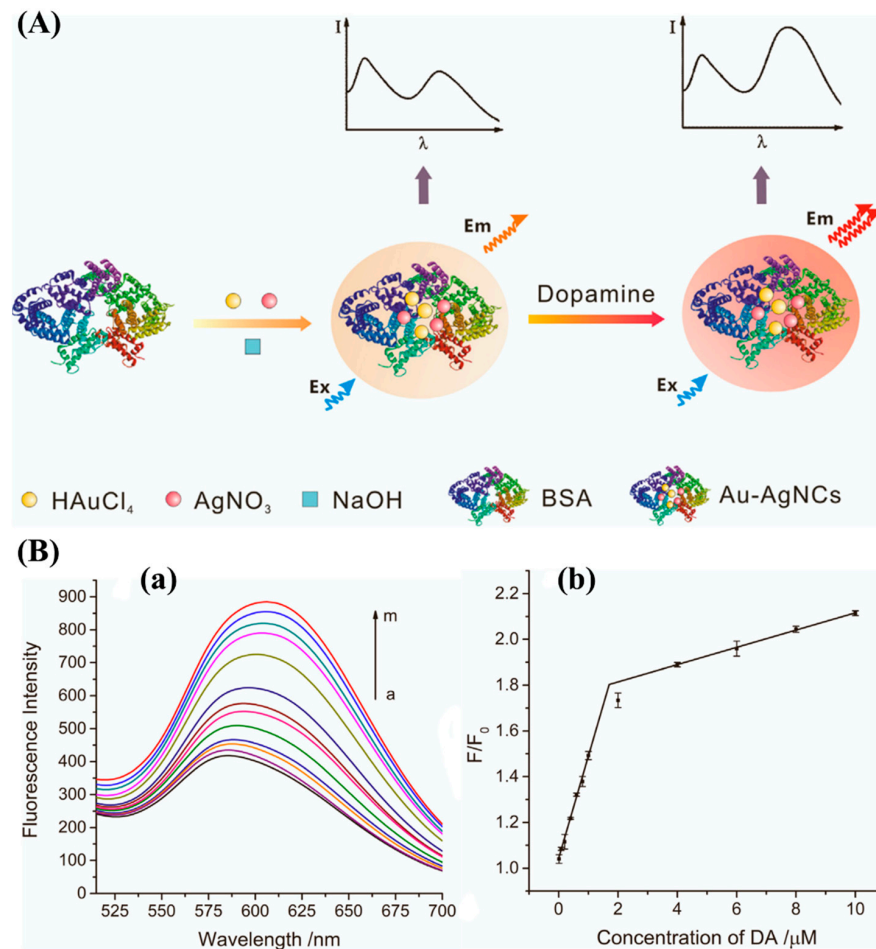


Figure 4. (A) Schematic diagram of bimetal Au-Ag nanocluster-based fluorescence detection of dopamine. (B) (a) Fluorescence intensity-correlated different concentrations of dopamine samples at 0, 0.01, 0.08, 0.2, 0.4, 0.6, 0.8, 1, 2, 4, 6, 8, and 10 μ M labeled from “a” to “m”. (b) A linear curve of fluorescence intensities correlated with the concentrations of dopamine at pH 8.5 Tris-HCl buffer. Fluorescence measurements under 370 nm excitation after 15 min incubations. Adapted from [84].

Figure 5 shows a dual-emissive AuNC-based sensor technique used for detecting 4-NP by means of fluorescence quenching. Herein, the first AuNCs were synthesized and stabilized by BSA to form the AuNCs@BSA complex. Subsequently, the inner filter effect (IFE), indicated that 4-NP selectively induced fluorescence quenching at 410 nm (F_{410}) of residual di-tyrosine (diTyr) more effectively than that at 630 nm (F_{630}) of AuNCs. Within 1 min, this sensor was successfully employed for trace detection of 4-NP by measuring the ratio of fluorescence intensity of F_{410}/F_{630} . Based on the 4-NP concentration-correlated ratio of F_{410}/F_{630} , its limit of detection was estimated at 13.8 nM (1.9 ng/mL). Furthermore, this technique shows highly sensitive and selective detection of 4-NP, despite the presence of eight other common phenol derivatives. Thus, this method was practically applied for an efficient analysis of trace 4-NP in actual river water samples [85].

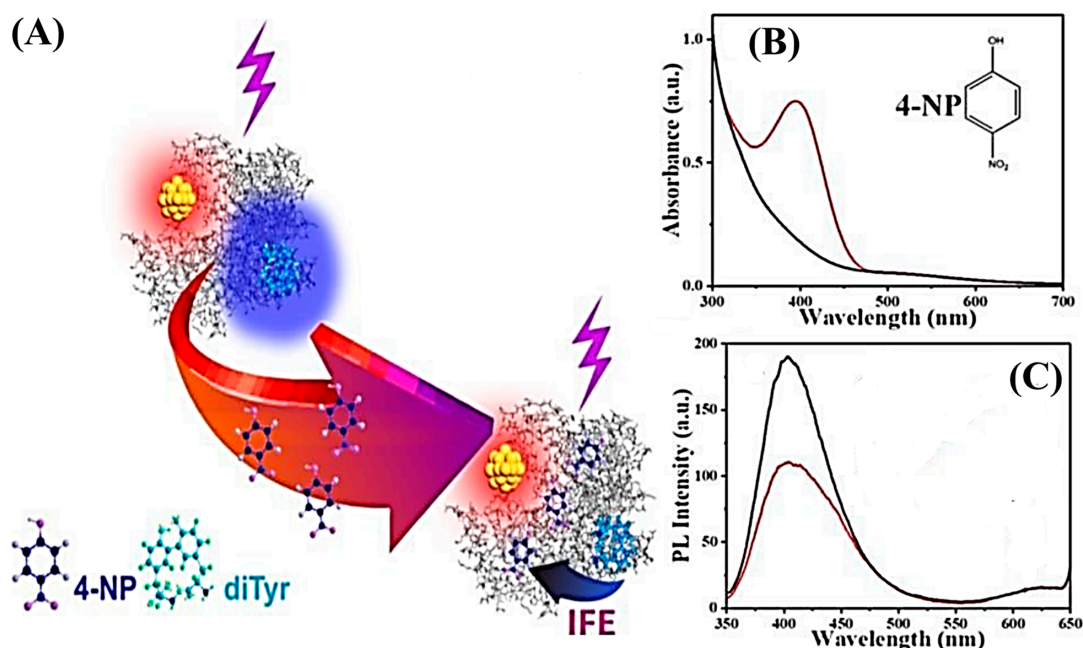


Figure 5. (A) Schematic illustration of AuNC-assisted and inner filter effect (IFE)-based fluorescence detection of 4-nitrophenol (4-NP) by means of selectively induced quenching of 410 nm fluorescence intensity of residual di-tyrosine (diTyr) using fluorescence intensity of AuNCs [85] at 630 nm in a complex of bovine serum albumin (BSA)-stabilized AuNCs. (B) UV/Vis spectroscopy of AuNCs@BSA before and after 4-NP addition, illustrated by a black line and a red line, respectively. (C) Under excitation at 330 nm, photoluminescent emission spectroscopy of AuNCs@BSA before and after 4-NP addition is demonstrated by a black line and a red line, respectively. Adapted from [85].

Other authors have successfully developed a novel Zn porphyrin MOF-based fluorescence sensor of bisphenol A detection using luminescence quenching. The experimental fluorescence data indicated that these MOF structures exhibited excellent monitoring of bisphenol A thanks to their electrostatic interaction, causing high sensitivity and selectivity in fluorescence quenching. In contrast, there was no significant quenching when the MOFs encountered the other phenolic substances, including *p*-cinnamyl phenol nonylphenol, octylphenol, 4-*tert*-butylphenol, 2,4-ditert-butylphenol, and diphenyl carbonate [86].

4. Localized Surface Plasmon Resonance Phenomenon-Based Optical Sensor for Phenolic Compounds

LSPR has been responsible for an enhanced electromagnetic field, inducing surface-enhanced spectroscopic technologies [87]. Several scientists are increasingly interested in plasmon resonance-based optical sensors, especially noble metal nanostructured materials such as Pt, Au, and Ag nanoparticles with various shapes and sizes, exhibiting plasmonic features that have been successfully used as a powerful analytic technique [6,88]. Here, these plasmonic nanostructures were practically employed as efficient transducers that convert changes in the spectral location of refractive index, thereby shifting the LSPR peak upon binding of analytes to either the surface of bare plasmonic nanostructures or specific receptor-conjugated nanomaterials. By coating unique probe molecules on the surface of plasmonic nanomaterials, LSPR-shift assay-based sensor techniques were introduced for specific analytics, considering a change in the signal localization of refractive index around their surfaces [89]. In addition, graphene oxide-based nanostructured hybrids have been successfully used as a novel material for enhanced SPR sensors thanks to their significant features, including strong adsorbed molecules, amplified signals, high electronic bridge, and simple fabrication. Moreover, regarding amplification of signals obtained by plasmonic materials, graphene-based nanostructure composites can significantly increase the sensitive detection of analytes up to fM [90]. Owing to their sensitivity and the selectivity of the spectral location of the refractive index, SPR-based optical sensors have been widely

investigated in sensing applications such as mercury ion detection [8,91], CO₂ detection [1], and gas sensors [2]. Some special emphasis on plasmonic nanostructures has been developed for the fabrication of novel surfaces, exposing high SPR-based optical sensors for phenolic compounds, such as GNP impregnation in TiO₂ structure-assisted hydroquinone detection [24], Au- and tyrosinase-modified graphene oxide film-introduced detection of phenol [9], and polymeric film-based phenol determination [92].

As shown in Figure 6A, an SPR-based optical sensor method was successfully implemented for dopamine detection based on a sensing layer of chitosan and graphene quantum dots, which were fabricated on Au thin film. The system of the SPR angle shift-based optical sensor showed a detection limit of 1.0 fM of dopamine [93]. In contrast, Figure 6B shows an innovative polyaniline/Pt-coated fiber optic-based SPR sensor used for ultra-sensitive detection of 4-nitrophenol, with a limit of detection of 0.34 pM [23].

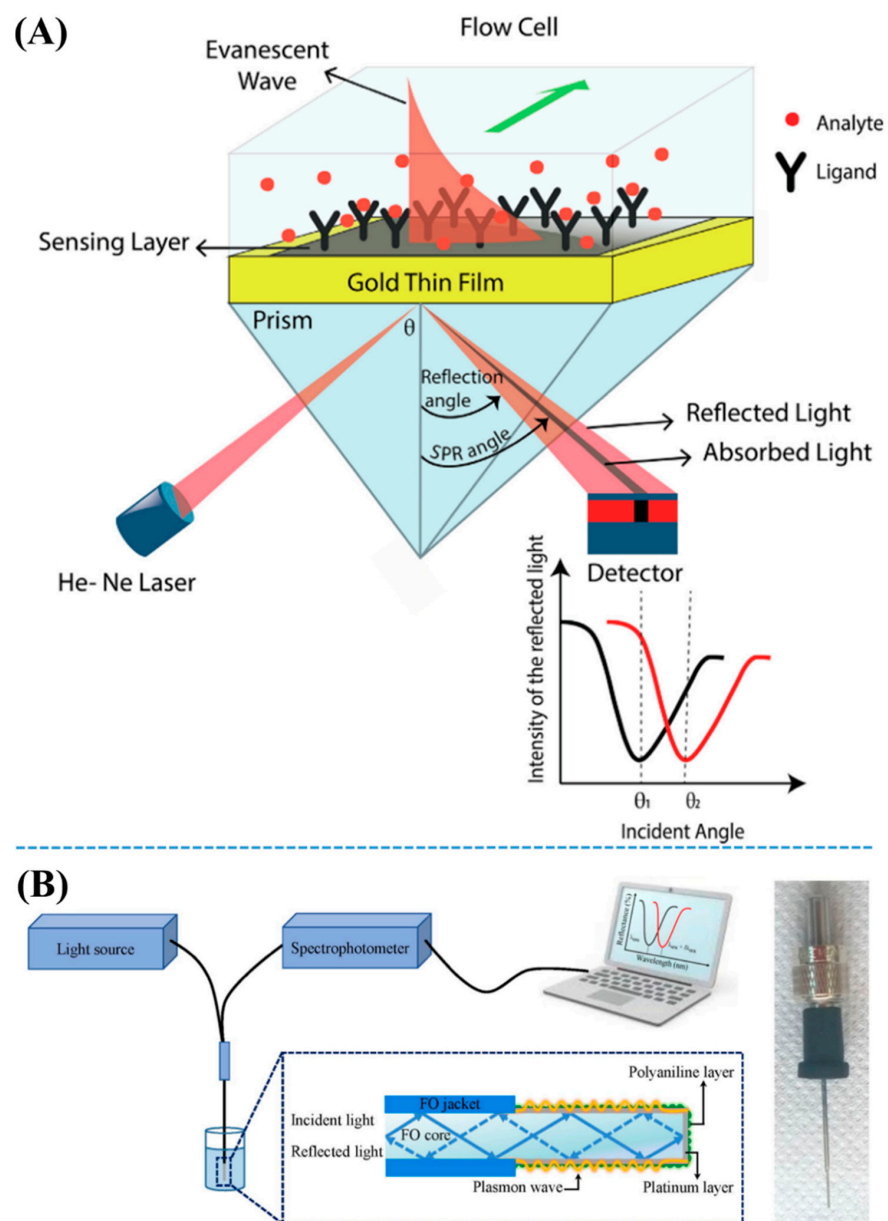


Figure 6. (A) Schematic diagram of dopamine detection using composites of chitosan/graphene quantum dots/Au thin film by means of SPR spectroscopy. Reproduced with permission from [93]. (B) Schematic diagram of 4-nitrophenol detection using innovative polyaniline/Pt-coated fiber optic-based SPR sensing substrate. Adapted from [23].

Recently, SPR-based sensor systems have also been introduced for application in photoelectrochemistry. Many scientists have investigated the optimized fabrication of new plasmonic nanomaterials, demonstrating unique features such as high and excellent plasmon enhancement as well as assistance for photoelectrochemical technologies. For example, there are several reports on Au-decorated $\text{La}_2\text{Ti}_2\text{O}_7/\text{rGO}$ -based plasmon enhancement-assisted photoelectrochemical monitoring of bisphenol A [94], SPR of GNP-activated $\text{g-C}_3\text{N}_4$ nanosheet-based photoelectrochemical determination of bisphenol A [95], and LSPR using carbon dot-functionalized GNPs for sensing of dopamine [96].

5. Plasmonic Resonance-Based Raman Sensors for Detection of Phenolic Compounds

Raman spectroscopic technologies—including micro-Raman mapping, imaging, and SERS spectroscopy—have been widely adopted in many fields such as food safety [97], the monitoring of contaminants [98], and the diagnosis of disease biomarkers [99]. Raman substrates may be divided by several kinds of pure noble metal nanostructured materials, hybrid nanomaterials, and MOF structures.

5.1. Pure Noble Metal Nanomaterial-Based Raman Sensors

Plasmonic nanostructured materials have been well known as one of the most significant keys leading to the success of sensing technologies thanks to their effective Raman-active substrates. Among various nanomaterials, Au and Ag as noble metals have been adapted as a potential platform, which has contributed to the sensitive Raman detection [5,100]. Furthermore, the unique shape and size of noble metals induce highly dense plasmonic hotspots to increase the sensitivity of the Raman method. Many scientists have discovered more novel structures of noble metals that aim to maximize the generation of a high density of plasmonic hotspots, inducing enhanced electromagnetic fields and amplified Raman signals. Besides the preparation of new structures, the modification of the surface of nanostructures were performed by specific probes for the sensitivity and selectivity of Raman sensing. For example, great efforts have been made toward this goal. AgNP-assisted Raman detection for bisphenol A determination [101] and GNP-induced Raman platforms for methyl parathion detection [102] have been considered.

Interestingly, Figure 7A shows SEM images of unique nanostructures of Ag nanorod bundles. Herein, Ag nanorods were well aligned as vertical bundles distributed on an Au/Cu template. This uniformity of Ag nanorod bundles demonstrates a potential application as a Raman-active platform used for trace detection of phenolic pollutants, including 4-chlorobiphenyl, methyl parathion, 2,4-dichlorophenoxyacetic acid (2,4-D), and two pesticides mixtures in water environments. Vertical bundles of Ag nanorod were well designed by combining porous anodic aluminum oxide membranes and spherical polystyrene templates. Based on the well-controlled ~ 65 nm diameter of AAO pores, the diameter of the Ag nanorods was also well achieved, such as the size of AAO pores. Figure 7A(a,b) show that vertical bundles of Ag-nanorod were well arranged with a $P6mm$ hexagonal symmetry. Each vertical bundle was surrounded by three other bundles and comprised an ~ 800 nm length size of 30–45 nanorods with a ~ 65 nm diameter (Figure 7A(c,d)). This unique structure exhibits a small gap (2 nm), leading to highly dense hot spots, inducing an enhanced Raman signal up to 10^8 . As shown in Figure 7B, to further illustrate the practical application of this Raman platform, vertical bundle arrays of Ag nanorods were used to detect phenolic pollutants of methyl parathion and 2,4-D in the environment using Raman spectroscopy, whose limits of detection were estimated as 21.5×10^{-9} M and 61.9×10^{-9} M, respectively [103].

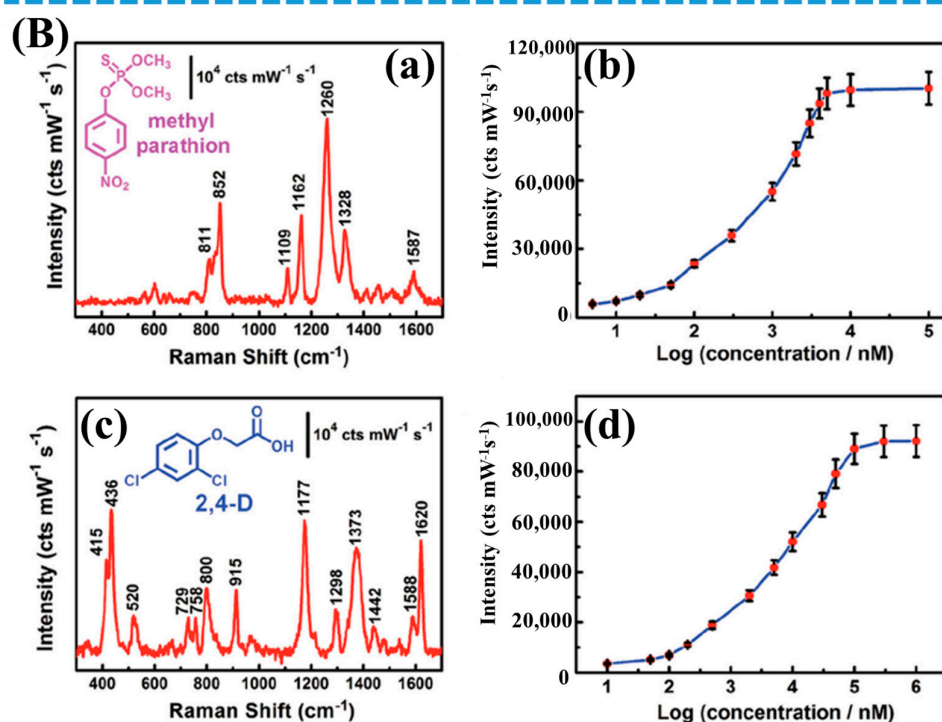
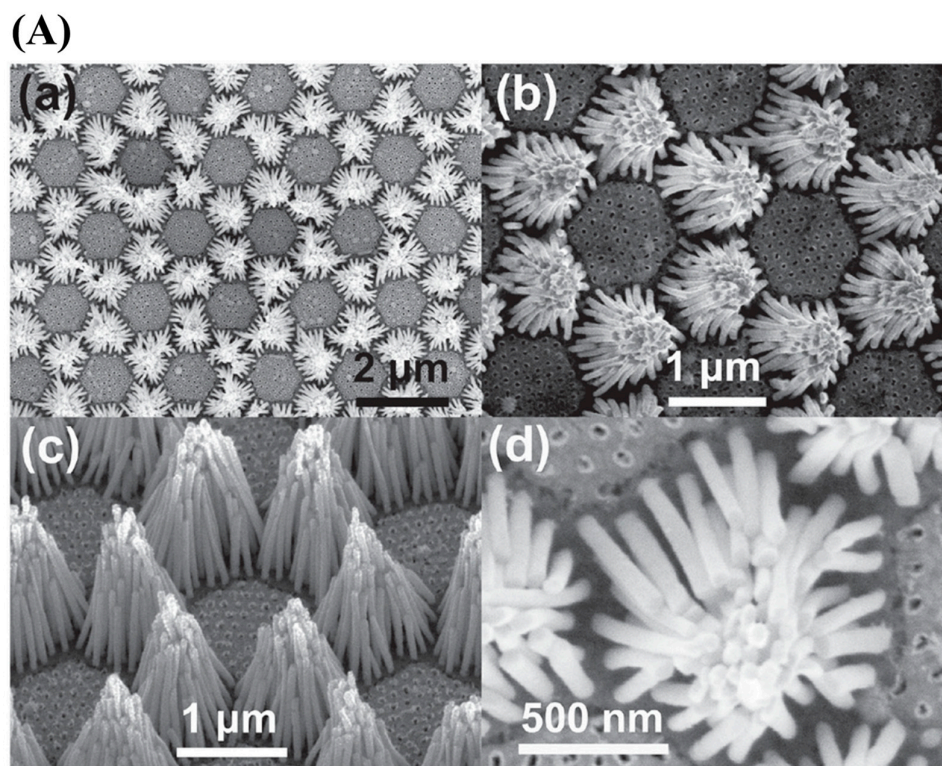


Figure 7. (A) SEM images of vertical bundles of Ag nanorods including top views with different scale bars of (a) 1 μm and (b) 2 μm , (c) side view of vertical bundle arrays of Ag nanorods, and (d) top view of one unique bundle of Ag-nanorods. (B) Vertical bundle arrays of Ag nanorod-based Raman detection of phenolic pollutants of (a) methyl parathion (0.3×10^{-6} M). (b) Linear curve of logarithmic concentration of methyl parathion-correlated Raman intensities (1260 cm^{-1}). (c) Raman spectra of 2,4-D (2×10^{-6} M). (d) Linear curve of logarithmic concentration of 2,4-D-correlated Raman intensities (1177 cm^{-1}). Adapted from [103].

An easy and rapid detection of bisphenol A detection has been successfully developed using Raman spectroscopy and a matrix of molecularly imprinted polymers (MIPs), where silver nanoparticles (AgNPs) were fabricated in situ inside this matrix. AgNPs have been well distributed in the matrix, leading to highly dense hotspots. Therefore, these Raman nanosensors of MIPs@AgNPs exhibit not only highly selective detection of bisphenol A in the presence of various similar molecules such as bisphenol AF and diethylstilbestrol, with an excellent detection limit as low as 5×10^{-8} M. Raman nanosensors exhibit the potential for practical applications with many benefits of easy fabrication, reusability, selectivity, and sensitive recognition [101].

Interestingly, Figure 8 demonstrates an AgNP-based microfluidic Raman biosensor for the highly sensitive detection of dopamine using DNA-assisted fabrication of ortho-nanodimers. Raman probes were modified with dopamine aptamers and 5,5'-dithiobis-(2-nitrobenzoic acid) (DTNB); these aptamers were well designed as unique zipper-like ortho-Ag nanodimers. Owing to the small gap in the specific zipper-like ortho-Ag nanodimers, the microfluidic Raman biosensor exhibited a highly targeted detection of dopamine, with a limit of detection as low as 10 aM [104].

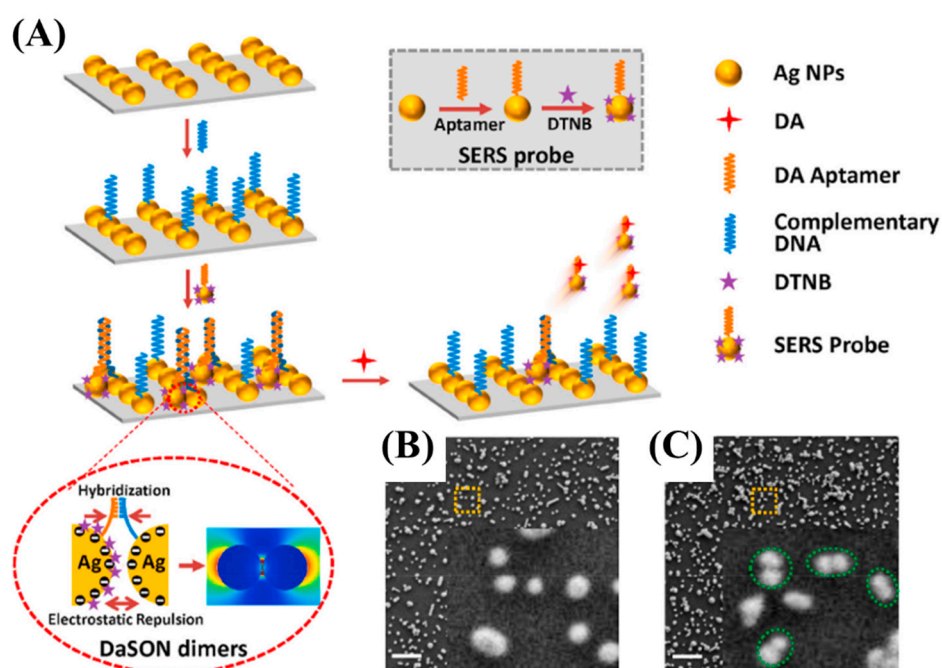


Figure 8. (A) Schematic diagram of Raman detection of dopamine (DA) using DNA-assisted synthesis of ortho-nanodimers (DaSON) of AgNPs. SEM images of Raman platforms with a scale bar of 500 nm (B) before and (C) after the adsorption of Raman probes containing DA aptamers and DTNB. Inserted pictures show an enlarged view of the yellow rectangle. Adapted from [104].

5.2. Hybrid Nanomaterial-Based Raman Sensors

As one of the most efficient plasmonic materials, hybrid nanomaterials—either bimetallic nanostructures or nanocomposites—have been widely adapted to prepare Raman substrates used in various fields as biosensors and environments. Recently, a novel Raman method has been developed to detect phenolic acids—vanillic acid, syringic acid, and gallic acid—using three-dimensional nanoprobles of a self-assembled composite of GNPs and SiO₂ [34]. In addition, AgNP-embedded poly (diallyl dimethyl-ammonium) chloride has been successfully used as a Raman substrate for biosensors, where this substrate was fabricated by modifying graphene oxide nanosheets. AgNPs have been well designed, yielding highly dense hotspots for enhanced Raman signals [105]. Owing to their excellent electromagnetic mechanism, bimetallic nanostructures have been used predominantly as biosensors, as shown in Figure 9.

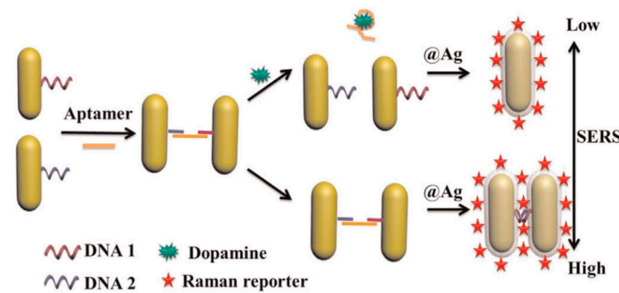


Figure 9. Schematic diagram of dopamine detection using bimetallic Au@Ag nanorod dimers, Raman reporter of 4-aminothiophenol, and aptamer. Adapted from [11].

Some authors have successfully self-assembled core–shell structured dimers of bimetallic Au@Ag nanorods, which were used as Raman nanosensors, particularly for detecting dopamine—a neurotransmitter—playing a key role in life. Based on aptamers and the electronic field of Ag shell coating outside the Au nanorod dimer, Raman signals have been well enhanced, indicating that the substrates exhibited an ultra-sensitive limit of dopamine detection at 0.006 pM [11]. As shown in Figure 10, Raman detection of chlorophenols was investigated by MIPs based on composites of SiO₂, rGO, and Au. Nanocomposite-based Raman have significantly enhanced signals, leading high sensitivity in chlorophenol detection [106]. Despite numerous efforts of Raman sensors based on plasmonic materials as nanostructures of noble metals and hybrids, more scientific studies are required to develop functional plasmonic nanostructured materials used for optical sensors. To understand plasmonic phenomena and interfaces of materials, some authors have discovered various MOF structures and revealed their effective ability for multi-detection of phenolic substances using SERS spectroscopy. In the next section, this review reveals several significant contributions to phenolic compound detection from MOF-assisted SERS sensors, according to some interesting examples.

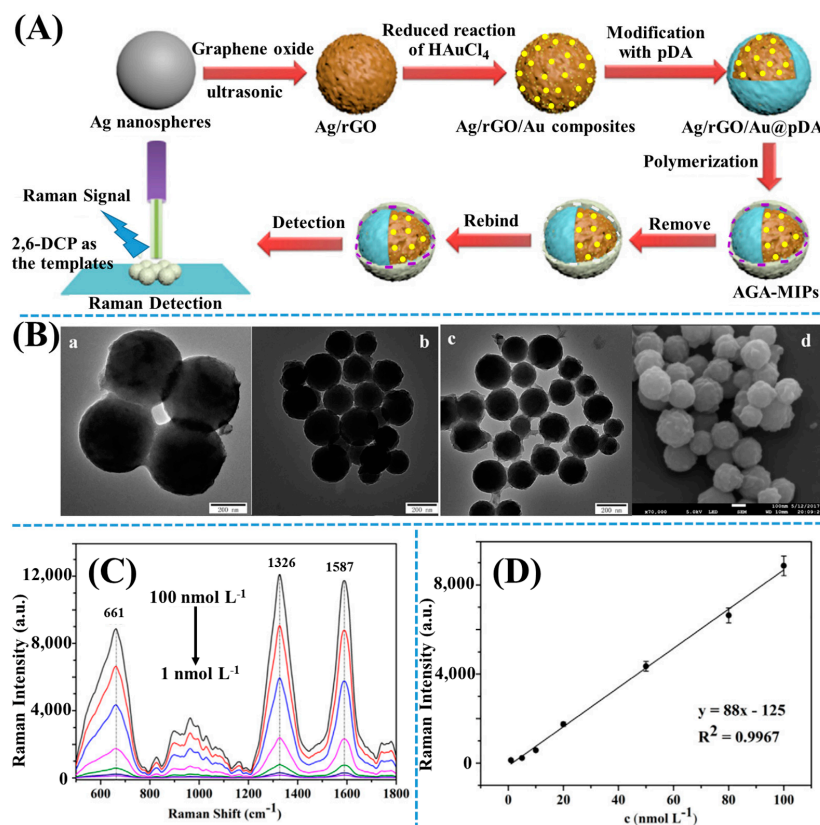


Figure 10. (A) Schematic diagram of trace detection of 2,6-DCP using Raman spectroscopy and MIPs based on nanocomposites of SiO₂/rGO/Au. (B) TEM images of (a) SiO₂/rGO, (b) composites

of polydopamine modified SiO₂/rGO/Au, (c) nanocomposites of SiO₂/rGO/Au, and (d) SEM image of SiO₂/rGO/Au nanocomposites. (C) Concentration-dependent Raman spectra of 2,6-DCP. (D) Linear curve of 2,6-DCP concentration-correlated Raman intensities at 661 cm⁻¹. Adapted from [106].

5.3. Metal–Organic Frameworks Structure-Introduced Raman Sensors

As shown in Figure 11A, a core–shell nanostructure of Cu₂O and SiO₂ was coated with ~4 nm porous Zn-based MOFs (ZIF-8) using an organic bridge as 5-mercapto-1-methyltetrazole, successfully yielding a novel Cu₂O@SiO₂@ZIF-8. Subsequently, in situ synthesis of AgNPs with various sizes from 2 nm to 29 nm on the surface of these MOFs was performed, inducing new MOFs and Cu₂O@SiO₂@ZIF-8@Ag. Owing to the strong interaction with ZIF-8, AgNPs were uniformly distributed in the structures of Cu₂O@SiO₂@ZIF-8. Interestingly, 4 nm AgNPs, assembled on Cu₂O@SiO₂@ZIF-8 templates, exhibited an excellent limit of detection, as low level as 5.76 × 10⁻¹² M concentration of phenol red in real samples. These Cu₂O@SiO₂@ZIF-8@Ag as 3D substrates could be employed for Raman monitoring of environmental contaminants [36]. Figure 11B shows the electromagnetic and chemical enhancement mechanisms of these Raman substrates. Firstly, owing to the many porous structures in Cu₂O@SiO₂@ZIF-8, AgNPs can be powerfully adsorbed and well loaded by the strong interaction with N and S atoms inside the ZIF-8 structure, thereby effectively preventing AgNP aggregation.

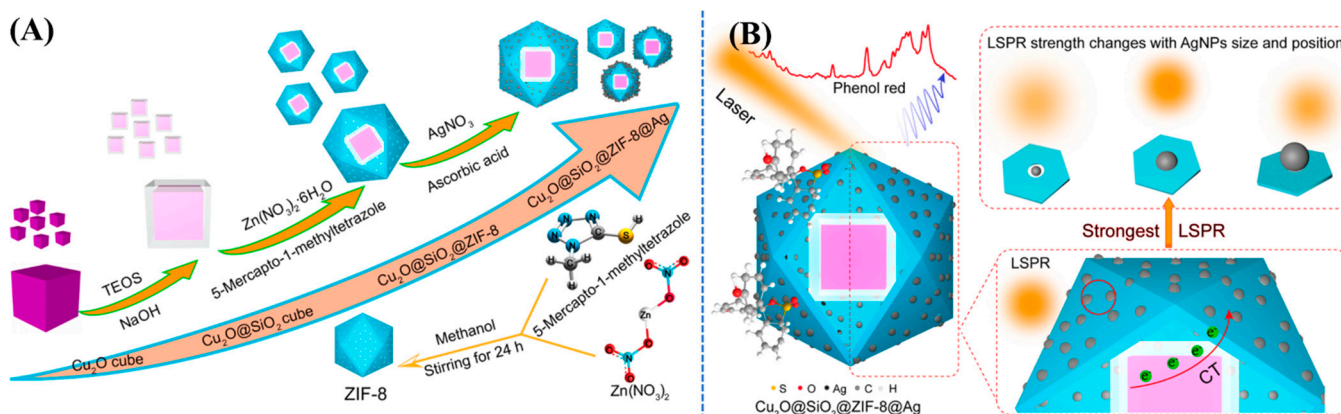


Figure 11. (A) Schematic diagram of the fabrication process of unique MOFs' structure as Cu₂O@SiO₂@ZIF-8@Ag. (B) Mechanism of Raman detection of phenol red using MOFs templates based on Cu₂O@SiO₂@ZIF-8@Ag. Adapted from [36].

Second, Cu₂O@SiO₂@ZIF-8@Ag exhibited a large surface area, assisting in the absorption of many phenol red molecules and strong binding between Ag and S atom via the Ag-S bond. However, owing to the high density of AgNPs on the surface of the MOF template, this SERS substrate generated many hotspots, enhancing Raman signals of phenol red that correspond to the electromagnetic mechanism. In contrast, charge transfer occurs as a result of the chemical enhancement mechanism between MOFs and phenol red molecules. Here, AgNPs provided an SPR phenomenon and encouraged charge transfer in the SERS system, increasing SERS signals. Importantly, a small size ~4 nm of AgNPs provides a maximum SERS signal of a MOF template because of more AgNPs located in porous ZIF-8. Nevertheless, different sizes of AgNPs will not properly match ZIF-8 pores, yielding weak Raman intensities [36].

As shown in Figure 12, the Raman sensor was combined with MIPs, inducing the distribution of a new Raman detection for selectivity of chloro-phenols. The Raman platforms as Ag@MIL-101(Fe)@MIPs were successfully fabricated by in situ synthesis of AgNPs on the surface of MOFs octahedral structures as MIL-101(Fe), subsequently, by polymerized precipitation between a template and a functional monomer as 2,6-DCP and acrylamide, respectively. MOF-based nanocomposite-assisted Raman monitoring of 2,6-

DCP with a limit of detection of 4.5 nmol/L. This method provides a potential Raman template not only for sensing other chlorophenols, but also for real sample analysis using Raman spectroscopy [42].

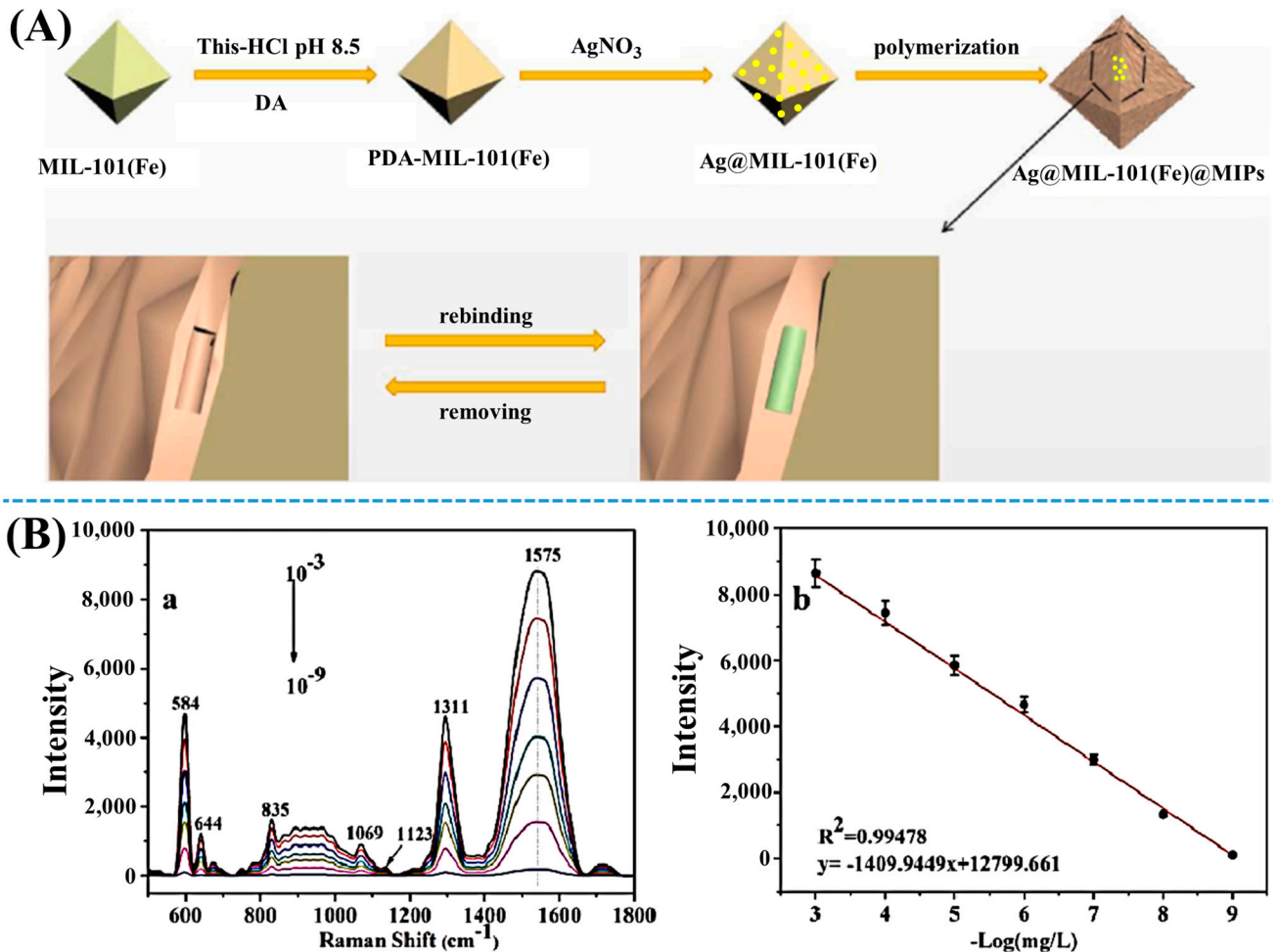


Figure 12. (A) Schematic diagram of the fabrication process of uniformed MOF structures of Ag@MIL-101 (Fe)@MIPs. (B) (a) MOF-based Raman spectra at different concentrations of 2,6-DCP. (b) A linear curve of logarithmic 2,6-DCP concentration-correlated Raman intensities at 1575 cm^{-1} . Adapted from [42].

As summarized in Table 1, based on plasmonic nanomaterials, numerous novel optical sensor technologies have been successfully developed for trace detection of phenol and phenolic compounds, with improvements in aspects such as selectivity and sensitivity as well as economical and reproducible benefits. The following aspects were studied and evaluated on the current spectroscopic and optical sensor methods. There are several perspectives to be addressed in future studies: (i) improving optical sensor methods based on pure, noble metal nanomaterials, and hybrid nanostructured materials; (ii) developing more MOFs that exhibit high target sensor; (iii) exhibiting the ability of multiple detections of similar analytes under various conditions; (iv) developing a dual functional sensing platform used for both Raman spectroscopy and fluorescence detection or both colorimetric and fluorescence; and (v) preparing a new nanomaterial that exhibits the ability of trace detection simultaneously and the removal of phenol and phenolic contaminants.

Table 1. Comparison of plasmonic resonance-based optical sensors for on-site detection of phenolic compounds.

Plasmonic Structures	Detection Methods	Target Compounds	Limit of Detection	Reference
Au-modified tyrosinase-based GO thin film	SPR	phenol	1 μ M	[9]
Au@Ag nanorod dimers	Raman	dopamine	0.006 pM	[11]
DNA-copper hybrid nanoflowers	colorimetric	dopamine	4.5 μ g/mL	[20]
		catechol	3.0 μ g/mL	
		hydroquinone	4.5 μ g/mL	
polyaniline/Pt-coated fiber optic	SPR	4-nitrophenol	0.34 pM	[23]
GNPs@TiO ₂	SPR	hydroquinone	33.8 nM	[24]
SiO ₂ /GNPs	Raman	vanillic acid	10–250 μ M	[34]
		syringic acid	10–110 μ M	
		gallic acid	5–55 μ M	
Cu ₂ O@SiO ₂ @ZIF-8@Ag	Raman	phenol red	5.76×10^{-12} M	[36]
Ag@MIL-101(Fe)@MIPs	Raman	2,6-dichlorophenol	4.5 nmol/L	[42]
		catechol	0.11 μ M	
		hydroquinone	1.6 μ M	
GNPs	colorimetric	phenol	1.02 μ M	[69]
		phenol	1.28 μ M	
Co-MOF-74-based Co ₃ O ₄ /cellulose	colorimetric	phenol	1.02 μ M	[69]
Zr(IV)-based MOFs	colorimetric	phenol	1.28 μ M	[70]
Adenosine monophosphate-Cu nanozymes	UV/Vis	phenolic compounds	0.033 μ mol/L	[71]
Au@Ni/rGO nanocomposite	colorimetric	phenol	1.68 μ M	[72]
Fe ₃ O ₄ /rGO/MOF	colorimetric	phenol	3.33×10^{-6} M	[73]
AgNPs	fluorescence	dopamine	5.3934×10^{-6} M	[80]
Au-Ag nanocluster	fluorescence	dopamine	6.9 nM	[84]
Au nanoclusters	fluorescence	4-nitrophenol	13.8 nM	[85]
chitosan/graphene quantum dots/Au thin film	SPR	dopamine	1.0 fM	[93]
carbon dot-functionalized GNPs	SPR	dopamine	0.23 μ M	[96]
GNPs	Raman	methyl parathion	0.011 μ g/cm ²	[102]
		methyl parathion	21.5×10^{-9} M	
		2,4-D	61.9×10^{-9} M	
zipper-like ortho-Ag nanodimers	Raman	dopamine	10 fM	[104]
AgNPs-graphene based nanosheets	Raman	<i>p</i> -cresol	10^{-5} M	[105]
SiO ₂ /rGO/Au	Raman	2,6-dichlorophenol	100–1.0 nM	[106]
Au-ZnO nanoparticle-modified tapered optical fiber	SPR	<i>p</i> -cresol	57.43 μ M	[107]
ZnO/MoS ₂	SPR	<i>p</i> -cresol	28 nM	[108]
cetyltrimethylammonium-bromide-functionalized ZnO/carbon nanotube nanocomposite coated over Ag film	plasmonic sensor	catechol	0.1 μ M	[109]

6. Conclusions

This review focused on recent developments in optical sensors, including colorimetric, fluorescence, LSPR, and plasmon-enhanced Raman scattering, used to determine phenol and phenolic compounds. Combined with numerous plasmonic nanomaterials such as noble metals, hybrids, and MOFs, these optical methods have been widely applied in many chemical and biological fields by improving sensing performance. Here, this review mainly discussed numerous novel designs of unique nanostructures, inducing enhanced signals, and selective sensing analytes. Among these optical sensors, colorimetric methods showed many benefits such as facile observation with the naked eyes, whereas the Raman method exhibited more selective molecular fingerprints. While the LSPR method revealed an excellent feature of high sensitivity, fluorescence assays showed an ultra-sensitive detection and limited stability for photo-bleaching. Notably, the development of plasmon resonance-based optical sensors for phenol detection indicates that future work would continue exploring superior nanomaterials for phenol determination with simpler manipulation, faster response, higher sensitivity, and better selectivity. We also believe that the combination of new plasmonic nanomaterials with traditional molecular design can improve sensing performance even further.

Author Contributions: Conceptualization, N.H.L., H.H.K. and S.J.S.; methodology, H.H.K.; resources, H.H.K.; data writing—original draft preparation, N.H.L.; writing—review and editing, S.J.S.; visualization, S.-W.J.; supervision, S.J.S. and S.-W.J. All authors have read and agreed to the published version of the manuscript.

Funding: Korea Ministry of Environment (MOE) as The Chemical Accident Prevention Technology Development Project and Korea Environment Industry and Technology Institute (KEITI) through Technology Development Project for Safety Management of Household Chemical Products Program, funded by the Korea Ministry of Environment (MOE) (2020002970005, 1485017845).

Institutional Review Board Statement: Not applicable.

Informed Consent Statement: Not applicable.

Data Availability Statement: Not applicable.

Conflicts of Interest: The authors declare no conflict of interest.

References

1. Pérez-Ocón, F.; Pozo, A.M.; Cortina, J.; Rabaza, O. Surface plasmon resonance sensor of CO₂ for indoors and outdoors. *Appl. Sci.* **2021**, *11*, 6869. [[CrossRef](#)]
2. Rodrigues, M.S.; Borges, J.; Lopes, C.; Pereira, R.M.S.; Vasilevskiy, M.I.; Vaz, F. Gas sensors based on localized surface plasmon resonances: Synthesis of oxide films with embedded metal nanoparticles, theory and simulation, and sensitivity enhancement strategies. *Appl. Sci.* **2021**, *11*, 5388. [[CrossRef](#)]
3. Zhang, L.; Chen, X.-R.; Wen, S.-H.; Liang, R.-P.; Qiu, J.-D. Optical sensors for inorganic arsenic detection. *TrAC Trends Anal. Chem.* **2019**, *118*, 869–879. [[CrossRef](#)]
4. Zhu, C.; Zhao, Q.; Wang, X.; Li, Z.; Hu, X. Ag-nanocubes/graphene-oxide/Au-nanoparticles composite film with highly dense plasmonic hotspots for surface-enhanced Raman scattering detection of pesticide. *Microchem. J.* **2021**, *165*, 106090. [[CrossRef](#)]
5. Omar, N.A.S.; Fen, Y.W.; Ramli, I.; Azmi, U.Z.M.; Hashim, H.S.; Abdullah, J.; Mahdi, M.A. Cellulose and vanadium plasmonic sensor to measure Ni²⁺ ions. *Appl. Sci.* **2021**, *11*, 2963. [[CrossRef](#)]
6. Nagy-Simon, T.; Hada, A.-M.; Suarasan, S.; Potara, M. Recent advances on the development of plasmon-assisted biosensors for detection of C-reactive protein. *J. Mol. Struct.* **2021**, *1246*, 131178. [[CrossRef](#)]
7. Varasteanu, P.; Kusko, M. A multi-objective optimization of 2D materials modified surface plasmon resonance (SPR) based sensors: An NSGA II approach. *Appl. Sci.* **2021**, *11*, 4353. [[CrossRef](#)]
8. Zhong, X.; Ma, L.; Yin, G.; Gan, M.; Wei, Y. Hg²⁺ optical fiber sensor based on LSPR with PDDA-templated AuNPs and CS/PAA bilayers. *Appl. Sci.* **2020**, *10*, 4845. [[CrossRef](#)]
9. Hashim, H.S.; Fen, Y.W.; Omar, N.A.S.; Abdullah, J.; Daniyal, W.M.E.M.M.; Saleviter, S. Detection of phenol by incorporation of gold modified-enzyme based graphene oxide thin film with surface plasmon resonance technique. *Opt. Express* **2020**, *28*, 9738–9752. [[CrossRef](#)]
10. Du, J.; Jing, C. One-step fabrication of dopamine-inspired Au for SERS sensing of Cd²⁺ and polycyclic aromatic hydrocarbons. *Anal. Chim. Acta* **2019**, *1062*, 131–139. [[CrossRef](#)]

11. Tang, L.; Li, S.; Han, F.; Liu, L.; Xu, L.; Ma, W.; Kuang, H.; Li, A.; Wang, L.; Xu, C. SERS-active Au@Ag nanorod dimers for ultrasensitive dopamine detection. *Biosens. Bioelectron.* **2015**, *71*, 7–12. [[CrossRef](#)] [[PubMed](#)]
12. Matteini, P.; Cottat, M.; Tavanti, F.; Panfilova, E.; Scuderi, M.; Nicotra, G.; Menziani, M.C.; Khlebtsov, N.; De Angelis, M.; Pini, R. Site-selective surface-enhanced Raman detection of proteins. *ACS Nano* **2017**, *11*, 918–926. [[CrossRef](#)] [[PubMed](#)]
13. Bhavya, M.B.; Prabhu, B.R.; Shenoy, B.M.; Bhol, P.; Swain, S.; Saxena, M.; John, N.S.; Hegde, G.; Samal, A.K. Femtomolar detection of thiram via SERS using silver nanocubes as an efficient substrate. *Environ. Sci. Nano* **2020**, *7*, 3999–4009. [[CrossRef](#)]
14. Lê, Q.T.; Ly, N.H.; Kim, M.-K.; Lim, S.H.; Son, S.J.; Zoh, K.-D.; Joo, S.-W. Nanostructured Raman substrates for the sensitive detection of submicrometer-sized plastic pollutants in water. *J. Hazard. Mater.* **2021**, *402*, 123499. [[CrossRef](#)] [[PubMed](#)]
15. Kim, N.; Ahn, Y.; Jo, J.; Pyo, H.; Lee, J.; Choi, J. Soil assessment after chemical accidents using metabolic profiling and microbial community evaluation. *Chemosphere* **2020**, *268*, 129362. [[CrossRef](#)] [[PubMed](#)]
16. Duan, W.; Meng, F.; Lin, Y.; Wang, G. Toxicological effects of phenol on four marine microalgae. *Environ. Toxicol. Pharmacol.* **2017**, *52*, 170–176. [[CrossRef](#)]
17. Duan, W.; Meng, F.; Cui, H.; Lin, Y.; Wang, G.; Wu, J. Ecotoxicity of phenol and cresols to aquatic organisms: A review. *Ecotoxicol. Environ. Saf.* **2018**, *157*, 441–456. [[CrossRef](#)] [[PubMed](#)]
18. Chae, Y.; Kim, L.; Kim, D.; Cui, R.; Lee, J.; An, Y.-J. Deriving hazardous concentrations of phenol in soil ecosystems using a species sensitivity distribution approach. *J. Hazard. Mater.* **2020**, *399*, 123036. [[CrossRef](#)]
19. Chandane, P.; Ladke, J.; Jori, C.; Deshmukh, S.; Zinjarde, S.; Chakankar, M.; Hocheng, H.; Jadhav, U. Synthesis of magnetic Fe₃O₄ nanoparticles from scrap iron and use of their peroxidase like activity for phenol detection. *J. Environ. Chem. Eng.* **2019**, *7*, 103083. [[CrossRef](#)]
20. Tran, T.D.; Nguyen, P.T.; Le, T.N.; Kim, M.I. DNA-copper hybrid nanoflowers as efficient laccase mimics for colorimetric detection of phenolic compounds in paper microfluidic devices. *Biosens. Bioelectron.* **2021**, *182*, 113187. [[CrossRef](#)]
21. Carvalho, D.G.; Ranzan, L.; Jacques, R.A.; Trierweiler, L.F.; Trierweiler, J.O. Analysis of total phenolic compounds and caffeine in teas using variable selection approach with two-dimensional fluorescence and infrared spectroscopy. *Microchem. J.* **2021**, *169*, 106570. [[CrossRef](#)]
22. Mainali, K.; Garcia-Perez, M. Identification and quantification of trace oxygenated compounds in alternative jet fuels: Fluorescence methods for fast detection of phenolic compounds in operational field conditions. *Fuel* **2020**, *271*, 117652. [[CrossRef](#)]
23. Antohe, I.; Iordache, I.; Antohe, V.-A.; Socol, G. A polyaniline/platinum coated fiber optic surface plasmon resonance sensor for picomolar detection of 4-nitrophenol. *Sci. Rep.* **2021**, *11*, 1–10. [[CrossRef](#)]
24. Mendonça, C.D.; Khan, S.U.; Rahemi, V.; Verbruggen, S.W.; Machado, S.A.S.; De Wael, K. Surface plasmon resonance-induced visible light photocatalytic TiO₂ modified with GNPs for the quantification of hydroquinone. *Electrochim. Acta* **2021**, *389*, 138734. [[CrossRef](#)]
25. Carreira-Casais, A.; Montes-García, V.; Pastoriza-Santos, I.; Prieto, M.; Simal-Gandara, J.; Pérez-Juste, J. Multiple SERS detection of phenol derivatives in tap water. *Proceedings* **2020**, *70*, 88. [[CrossRef](#)]
26. Dendisová, M.; Němečková, Z.; Člupek, M.; Prokopec, V. EC-SERS study of phenolic acids sorption behavior on Au, Ag and Cu substrates—Effect of applied potential and metal used. *Appl. Surf. Sci.* **2019**, *470*, 716–723. [[CrossRef](#)]
27. Deneva, V.; Bakardzhiyski, I.; Bambalov, K.; Antonova, D.; Tsobanova, D.; Bambalov, V.; Cozzolino, D.; Antonov, L. Using Raman spectroscopy as a fast tool to classify and analyze Bulgarian wines—A feasibility study. *Molecules* **2019**, *25*, 170. [[CrossRef](#)] [[PubMed](#)]
28. Wang, J.; Qiu, C.; Mu, X.; Pang, H.; Chen, X.; Liu, D. Ultrasensitive SERS detection of rhodamine 6G and *p*-nitrophenol based on electrochemically roughened nano-Au film. *Talanta* **2020**, *210*, 120631. [[CrossRef](#)]
29. Wan, M.; Zhao, H.; Wang, Z.; Zou, X.; Zhao, Y.; Sun, L. Fabrication of Ag modified SiO₂ electrospun nanofibrous membranes as ultrasensitive and high stable SERS substrates for multiple analytes detection. *Colloids Interface Sci. Commun.* **2021**, *42*, 100428. [[CrossRef](#)]
30. Sun, J.; Xue, D.; Shan, W.; Liu, R.; Liu, R.; Zhao, H.; Li, T.; Wang, Z.; Zhang, J.; Shao, B. In situ growth large area silver nanostructure on metal phenolic network coated NAAO film and its SERS sensing application for monofluoroacetic acid. *ACS Sens.* **2021**, *6*, 2129–2135. [[CrossRef](#)]
31. Sricharoen, N.; Sukmanee, T.; Pienpinijtham, P.; Ekgasit, S.; Kitahama, Y.; Ozaki, Y.; Wongravee, K. MCR-ALS with sample insertion constraint to enhance the sensitivity of surface-enhanced Raman scattering detection. *Analyst* **2021**, *146*, 3251–3262. [[CrossRef](#)] [[PubMed](#)]
32. Shen, Y.; Yu, D.; Han, F.-Y.; Shen, A.-G.; Hu, J.-M. On-site and quantitative SERS detection of trace 1,2,3-benzotriazole in transformer oil with colloidal lignin particles-based green pretreatment reagents. *Spectrochim. Acta A Mol. Biomol. Spectrosc.* **2021**, *252*, 119469. [[CrossRef](#)] [[PubMed](#)]
33. Rostami, S.; Zór, K.; Zhai, D.S.; Viehrig, M.; Morelli, L.; Mehdinia, A.; Smedsgaard, J.; Rindzevicius, T.; Boisen, A. High-throughput label-free detection of Ochratoxin A in wine using supported liquid membrane extraction and Ag-capped silicon nanopillar SERS substrates. *Food Control* **2020**, *113*, 107183. [[CrossRef](#)]
34. Rao, Y.; Zhao, X.; Li, Z.; Huang, J. Phenolic acids induced growth of 3D ordered gold nanoshell composite array as sensitive SERS nanosensor for antioxidant capacity assay. *Talanta* **2018**, *190*, 174–181. [[CrossRef](#)] [[PubMed](#)]

35. Aarathi, A.; Bindhu, M.; Umadevi, M.; Parimaladevi, R.; Sathe, G.; Al-Mohaimed, A.M.; Elshikh, M.S.; Balasubramanian, B. Evaluating the detection efficacy of advanced bimetallic plasmonic nanoparticles for heavy metals, hazardous materials and pesticides of leachate in contaminated groundwater. *Environ. Res.* **2021**, *201*, 111590. [[CrossRef](#)]
36. Chen, X.; Qin, L.; Kang, S.-Z.; Li, X. A special zinc metal-organic frameworks-controlled composite nanosensor for highly sensitive and stable SERS detection. *Appl. Surf. Sci.* **2021**, *550*, 149302. [[CrossRef](#)]
37. Xu, J.; Shang, S.; Gao, W.; Zeng, P.; Jiang, S. Ag@ZIF-67 decorated cotton fabric as flexible, stable and sensitive SERS substrate for label-free detection of phenol-soluble modulin. *Cellulose* **2021**, *28*, 1–16. [[CrossRef](#)]
38. Heredia-Cancino, J.A.; Carrillo-Torres, R.C.; Félix-Domínguez, F.; Álvarez-Ramos, M.E. Experimental characterization of chemical properties of engine oil using localized surface plasmon resonance sensing. *Appl. Sci.* **2021**, *11*, 8518. [[CrossRef](#)]
39. Hashim, H.S.; Fen, Y.W.; Omar, N.A.S.; Fauzi, N.I.M.; Daniyal, W.M.E.M.M. Recent advances of priority phenolic compounds detection using phenol oxidases-based electrochemical and optical sensors. *Measurement* **2021**, *184*, 109855. [[CrossRef](#)]
40. Tarafdar, A.; Sirohi, R.; Balakumaran, P.A.; Reshmy, R.; Madhavan, A.; Sindhu, R.; Binod, P.; Kumar, Y.; Kumar, D.; Sim, S.J. The hazardous threat of Bisphenol A: Toxicity, detection and remediation. *J. Hazard. Mater.* **2022**, *423*, 127097. [[CrossRef](#)]
41. Ullah, R.; Wang, X. Raman spectroscopy of bisphenol 'S' and its analogy with bisphenol 'A' uncovered with a dimensionality reduction technique. *J. Mol. Struct.* **2019**, *1175*, 927–934. [[CrossRef](#)]
42. Zhang, J.; Wang, D.; Li, Y.; Wang, J.; Bai, D.; Zhou, C.; He, J.; Shi, S.; Li, H. Construction of octahedral SERS blotting imprinted sensor for selective detection of 2,6-dichlorophenol. *Opt. Mater.* **2021**, *112*, 110764. [[CrossRef](#)]
43. Albuquerque, B.R.; Heleno, S.A.; Oliveira, M.B.P.P.; Barros, L.; Ferreira, I.C.F.R. Phenolic compounds: Current industrial applications, limitations and future challenges. *Food Funct.* **2021**, *12*, 14–29. [[CrossRef](#)] [[PubMed](#)]
44. Kumar, N.; Goel, N. Phenolic acids: Natural versatile molecules with promising therapeutic applications. *Biotechnol. Rep.* **2019**, *24*, e00370. [[CrossRef](#)]
45. Arfin, T.; Sonawane, K.; Tarannum, A. Review on detection of phenol in water. *Adv. Mater. Lett.* **2019**, *10*, 753–785. [[CrossRef](#)]
46. Javaid, S.; Lee, J.; Sofianos, M.V.; Douglas-Moore, Z.; Arrigan, D.W.M.; Silvester, D.S. Zinc oxide nanoparticles as antifouling materials for the electrochemical detection of methylparaben. *ChemElectroChem* **2021**, *8*, 187–194. [[CrossRef](#)]
47. Rahman, M.M.; Alam, M.M.; Asiri, A.M. Development of an efficient phenolic sensor based on facile Ag₂O/Sb₂O₃ nanoparticles for environmental safety. *Nanoscale Adv.* **2019**, *1*, 696–705. [[CrossRef](#)]
48. Romih, T.; Menart, E.; Jovanovski, V.; Jerič, A.; Andrenšek, S.; Hočevar, S.B. Sodium-polyacrylate-based electrochemical sensors for highly sensitive detection of gaseous phenol at room temperature. *ACS Sens.* **2020**, *5*, 2570–2577. [[CrossRef](#)]
49. Fu, S.; Zhu, Y.; Zhang, Y.; Zhang, M.; Zhang, Y.; Qiao, L.; Yin, N.; Song, K.; Liu, M.; Wang, D. Recent advances in carbon nanomaterials-based electrochemical sensors for phenolic compounds detection. *Microchem. J.* **2021**, *171*, 106776. [[CrossRef](#)]
50. Ayhan, N.K.; Rosenberg, E. Development of comprehensive liquid chromatography with diode array and mass spectrometric detection for the characterization of (poly-)phenolic and flavonoid compounds and application to asparagus. *Food Chem.* **2021**, *354*, 129518. [[CrossRef](#)]
51. Liu, W.; Xie, M.; Hao, X.; Xu, Q.; Jiang, X.; Liu, T.; Wang, M. Rapid synergistic cloud point extraction for simultaneous determination of five polar phenols in environmental water samples via high performance liquid chromatography with fluorescence detection. *Microchem. J.* **2021**, *164*, 105963. [[CrossRef](#)]
52. Luo, X.; Zheng, H.; Zhang, Z.; Wang, M.; Yang, B.; Huang, L.; Wang, M. Cloud point extraction for simultaneous determination of 12 phenolic compounds by high performance liquid chromatography with fluorescence detection. *Microchem. J.* **2018**, *137*, 148–154. [[CrossRef](#)]
53. Kolahchi, N.; Braiek, M.; Ebrahimipour, G.; Ranaei-Siadat, S.O.; Lagarde, F.; Jaffrezic-Renault, N. Direct detection of phenol using a new bacterial strain-based conductometric biosensor. *J. Environ. Chem. Eng.* **2018**, *6*, 478–484. [[CrossRef](#)]
54. Li, K.; Yang, Y.; Bacha, A.-U.-R.; Feng, Y.; Ajmal, S.; Nabi, I.; Zhang, L. Efficiently complete degradation of 2,4-DCP using sustainable photoelectrochemical reduction and sequential oxidation method. *Chem. Eng. J.* **2019**, *378*, 122191. [[CrossRef](#)]
55. Shahbakhsh, M.; Saravani, H.; Narouie, S.; Hashemzaei, Z. Poly (hydroquinone-oxovanadium (IV)) porous hollow microspheres for voltammetric detection of phenol. *Microchem. J.* **2021**, *164*, 105948. [[CrossRef](#)]
56. Yi, Z.; Kun-Lin, Y. Quantitative detection of phenol in wastewater using square wave voltammetry with pre-concentration. *Anal. Chim. Acta* **2021**, *1178*, 338788. [[CrossRef](#)]
57. Li, D.; Cheng, Y.; Zuov, H.; Zhang, W.; Pan, G.; Fu, Y.; Wei, Q. Dual-functional biocatalytic membrane containing laccase-embedded metal-organic frameworks for detection and degradation of phenolic pollutant. *J. Colloid Interface Sci.* **2021**, *603*, 771–782. [[CrossRef](#)]
58. Della Pelle, F.; Compagnone, D. Nanomaterial-based sensing and biosensing of phenolic compounds and related antioxidant capacity in food. *Sensors* **2018**, *18*, 462. [[CrossRef](#)]
59. Li, N.; Chen, H.; Zhang, M.; Zha, Y.; Mu, Z.; Ma, Y.; Chen, P. A universal ultrasensitive platform for enzyme-linked immunoassay based on responsive surface-enhanced Raman scattering. *Sens. Actuators B Chem.* **2020**, *315*, 128135. [[CrossRef](#)]
60. Hariharan, A.; Chelli, S.M.; Belliraj, S.K.; Ferrari, M.; Narasimha, N.K.; Vishnubhatla, K.C. Paper-microfluidics based SERS substrate for PPB level detection of catechol. *Opt. Mater.* **2019**, *94*, 305–310. [[CrossRef](#)]
61. Li, D.; Li, D.-W.; Fossey, J.S.; Long, Y.-T. Portable surface-enhanced Raman scattering sensor for rapid detection of aniline and phenol derivatives by on-site electrostatic preconcentration. *Anal. Chem.* **2010**, *82*, 9299–9305. [[CrossRef](#)]

62. Yu, J.; Tsow, F.; Mora, S.J.; Tipparaju, V.V.; Xian, X. Hydrogel-incorporated colorimetric sensors with high humidity tolerance for environmental gases sensing. *Sens. Actuators B Chem.* **2021**, *345*, 130404. [[CrossRef](#)] [[PubMed](#)]
63. Tang, Y.; Huang, X.; Wang, X.; Wang, C.; Tao, H.; Wu, Y. G-quadruplex DNAzyme as peroxidase mimetic in a colorimetric biosensor for ultrasensitive and selective detection of trace tetracyclines in foods. *Food Chem.* **2022**, *366*, 130560. [[CrossRef](#)] [[PubMed](#)]
64. Alkasir, R.S.J.; Ornatska, M.; Andreescu, S. Colorimetric paper bioassay for the detection of phenolic compounds. *Anal. Chem.* **2012**, *84*, 9729–9737. [[CrossRef](#)] [[PubMed](#)]
65. Zhang, L.-P.; Xing, Y.-P.; Liu, L.-H.; Zhou, X.-H.; Shi, H.-C. Fenton reaction-triggered colorimetric detection of phenols in water samples using unmodified gold nanoparticles. *Sens. Actuators B Chem.* **2016**, *225*, 593–599. [[CrossRef](#)]
66. Zhang, D.; Yang, J.; Ye, J.; Xu, L.; Xu, H.; Zhan, S.; Xia, B.; Wang, L. Colorimetric detection of bisphenol A based on unmodified aptamer and cationic polymer aggregated gold nanoparticles. *Anal. Biochem.* **2016**, *499*, 51–56. [[CrossRef](#)]
67. Jia, M.; Sha, J.; Li, Z.; Wang, W.; Zhang, H. High affinity truncated aptamers for ultra-sensitive colorimetric detection of bisphenol A with label-free aptasensor. *Food Chem.* **2020**, *317*, 126459. [[CrossRef](#)] [[PubMed](#)]
68. Feng, Y.; Wang, Y.; Ying, Y. Structural design of metal–organic frameworks with tunable colorimetric responses for visual sensing applications. *Coord. Chem. Rev.* **2021**, *446*, 214102. [[CrossRef](#)]
69. Hou, C.; Fu, L.; Wang, Y.; Chen, W.; Chen, F.; Zhang, S.; Wang, J. Co-MOF-74 based Co₃O₄/cellulose derivative membrane as dual-functional catalyst for colorimetric detection and degradation of phenol. *Carbohydr. Polym.* **2021**, *273*, 118548. [[CrossRef](#)]
70. Wang, J.; Zhou, Y.; Zeng, M.; Zhao, Y.; Zuo, X.; Meng, F.; Lv, F.; Lu, Y. Zr(IV)-based metal-organic framework nanocomposites with enhanced peroxidase-like activity as a colorimetric sensing platform for sensitive detection of hydrogen peroxide and phenol. *Environ. Res.* **2022**, *203*, 111818. [[CrossRef](#)]
71. Huang, H.; Lei, L.; Bai, J.; Zhang, L.; Song, D.; Zhao, J.; Li, J.; Li, Y. Efficient elimination and detection of phenolic compounds in juice using laccase mimicking nanozymes. *Chin. J. Chem. Eng.* **2021**, *29*, 167–175. [[CrossRef](#)]
72. Darabdhara, G.; Das, M.R. Dual responsive magnetic Au@Ni nanostructures loaded reduced graphene oxide sheets for colorimetric detection and photocatalytic degradation of toxic phenolic compounds. *J. Hazard. Mater.* **2019**, *368*, 365–377. [[CrossRef](#)] [[PubMed](#)]
73. Wang, Y.; Zhao, M.; Hou, C.; Yang, X.; Li, Z.; Meng, Q.; Liang, C. Graphene-based magnetic metal organic framework nanocomposite for sensitive colorimetric detection and facile degradation of phenol. *J. Taiwan Inst. Chem. Eng.* **2019**, *102*, 312–320. [[CrossRef](#)]
74. Li, M.; Lei, P.; Song, S.; Shuang, S.; Wang, R.; Dong, C. A butterfly-shaped ESIPT molecule with solid-state fluorescence for the detection of latent fingerprints and exogenous and endogenous ONOO[−] by caging of the phenol donor. *Talanta* **2021**, *233*, 122593. [[CrossRef](#)] [[PubMed](#)]
75. Balijapalli, U.; Manickam, S.; Thirumoorthy, K.; Sundaramoorthy, K.N.; Sathiyarayanan, K.I. (Tetrahydrodibenzo[a,i]phenanthridin-5-yl)phenol as a fluorescent probe for the detection of aniline. *J. Org. Chem.* **2019**, *84*, 11513–11523. [[CrossRef](#)]
76. Grzelakowska, A.; Zielonka, M.; Dębowska, K.; Modrzejewska, J.; Szala, M.; Sikora, A.; Zielonka, J.; Podsiadły, R. Two-photon fluorescent probe for cellular peroxynitrite: Fluorescence detection, imaging, and identification of peroxynitrite-specific products. *Free Radic. Biol. Med.* **2021**, *169*, 24–35. [[CrossRef](#)] [[PubMed](#)]
77. Zeng, L.; Zhang, X.; Wang, X.; Cheng, D.; Li, R.; Han, B.; Wu, M.; Zhuang, Z.; Ren, A.; Zhou, Y.; et al. Simultaneous fluorescence determination of bisphenol A and its halogenated analogs based on a molecularly imprinted paper-based analytical device and a segment detection strategy. *Biosens. Bioelectron.* **2021**, *180*, 113106. [[CrossRef](#)]
78. Santos, I.; Bosman, G.; Aleixandre-Tudo, J.L.; du Toit, W. Direct quantification of red wine phenolics using fluorescence spectroscopy with chemometrics. *Talanta* **2022**, *236*, 122857. [[CrossRef](#)]
79. Liu, L.; Zhao, Q. A simple fluorescence anisotropy assay for detection of bisphenol A using fluorescently labeled aptamer. *J. Environ. Sci.* **2020**, *97*, 19–24. [[CrossRef](#)]
80. Sivakumar, P.; Priyatharshni, S.; Kumar, K. Fluorescent silver nanoparticles for sensitive and selective detection of dopamine. *Mater. Chem. Phys.* **2020**, *240*, 122167. [[CrossRef](#)]
81. Pan, Y.; Wei, X.; Guo, X.; Wang, H.; Song, H.; Pan, C.; Xu, N. Immunoassay based on Au-Ag bimetallic nanoclusters for colorimetric/fluorescent double biosensing of dicofol. *Biosens. Bioelectron.* **2021**, *194*, 113611. [[CrossRef](#)] [[PubMed](#)]
82. Li, M.; Zhu, N.; Zhu, W.; Zhang, S.; Li, F.; Wu, P.; Li, X. Enhanced emission and higher stability ovalbumin-stabilized gold nanoclusters (OVA-AuNCs) modified by polyethyleneimine for the fluorescence detection of tetracyclines. *Microchem. J.* **2021**, *169*, 106560. [[CrossRef](#)]
83. Kamel, R.M.; Mohamed, S.K. Highly sensitive solid-state fluorescent sensor immobilized on silica nanoparticles for direct detection dimethyl phenol in seawater samples. *J. Mol. Struct.* **2021**, *1246*, 131128. [[CrossRef](#)]
84. Zhou, T.; Su, Z.; Tu, Y.; Yan, J. Determination of dopamine based on its enhancement of gold-silver nanocluster fluorescence. *Spectrochim. Acta A Mol. Biomol. Spectrosc.* **2021**, *252*, 119519. [[CrossRef](#)] [[PubMed](#)]
85. Shu, T.; Wang, J.; Lin, X.; Zhou, Z.; Liang, F.; Su, L.; Zhang, X. Dual-emissive gold nanoclusters for label-free and separation-free ratiometric fluorescence sensing of 4-nitrophenol based on the inner filter effect. *J. Mater. Chem. C* **2018**, *6*, 5033–5038. [[CrossRef](#)]
86. Pang, Y.; Cao, Y.; Han, J.; Xia, Y.; He, Z.; Sun, L.; Liang, J. A novel fluorescence sensor based on Zn porphyrin MOFs for the detection of bisphenol A with highly selectivity and sensitivity. *Food Control* **2022**, *132*, 108551. [[CrossRef](#)]

87. Willets, K.A.; Van Duyne, R.P. Localized surface plasmon resonance spectroscopy and sensing. *Annu. Rev. Phys. Chem.* **2007**, *58*, 267–297. [[CrossRef](#)]
88. Yazdian-Robati, R.; Hedayati, N.; Dehghani, S.; Ramezani, M.; Alibolandi, M.; Saeedi, M.; Abnous, K.; Taghdisi, S.M. Application of the catalytic activity of gold nanoparticles for development of optical aptasensors. *Anal. Biochem.* **2021**, *629*, 114307. [[CrossRef](#)]
89. Szunerits, S.; Boukherroub, R. Sensing using localised surface plasmon resonance sensors. *Chem. Commun.* **2012**, *48*, 8999–9010. [[CrossRef](#)]
90. Patil, P.O.; Pandey, G.R.; Patil, A.G.; Borse, V.B.; Deshmukh, P.K.; Patil, D.R.; Tade, R.S.; Nangare, S.N.; Khan, Z.G.; Patil, A.M.; et al. Graphene-based nanocomposites for sensitivity enhancement of surface plasmon resonance sensor for biological and chemical sensing: A review. *Biosens. Bioelectron.* **2019**, *139*, 111324. [[CrossRef](#)]
91. Ramdzan, N.S.M.; Fen, Y.W.; Omar, N.A.S.; Anas, N.A.A.; Liew, J.Y.C.; Daniyal, W.M.E.M.M.; Hashim, H.S. Detection of mercury ion using surface plasmon resonance spectroscopy based on nanocrystalline cellulose/poly(3,4-ethylenedioxythiophene) thin film. *Measurement* **2021**, *182*, 109728. [[CrossRef](#)]
92. Derazshamshir, A. Preparation of molecularly imprinted optical sensors for the real time detection of phenol. *Hacettepe J. Biol. Chem.* **2021**, *49*, 333–344. [[CrossRef](#)]
93. Eddin, F.B.K.; Fen, Y.W.; Omar, N.A.S.; Liew, J.Y.C.; Daniyal, W.M.E.M.M. Femtomolar detection of dopamine using surface plasmon resonance sensor based on chitosan/graphene quantum dots thin film. *Spectrochim. Acta A Mol. Biomol. Spectrosc.* **2021**, *263*, 120202. [[CrossRef](#)] [[PubMed](#)]
94. Zhang, L.; Zhang, H.; Chen, Q.; Zhai, C. Plasmon enhanced photo-assisted electrochemical detection of bisphenol A based on Au decorated La₂Ti₂O₇/RGO nanosheets. *Surf. Interfaces* **2021**, *26*, 101331. [[CrossRef](#)]
95. Deiminiat, B.; Rounaghi, G.H. A novel visible light photoelectrochemical aptasensor for determination of bisphenol A based on surface plasmon resonance of gold nanoparticles activated g-C₃N₄ nanosheets. *J. Electroanal. Chem.* **2021**, *886*, 115122. [[CrossRef](#)]
96. Amiri, M.; Dadfarnia, S.; Shabani, A.M.H.; Sadjadi, S. Non-enzymatic sensing of dopamine by localized surface plasmon resonance using carbon dots-functionalized gold nanoparticles. *J. Pharm. Biomed. Anal.* **2019**, *172*, 223–229. [[CrossRef](#)] [[PubMed](#)]
97. Petersen, M.; Yu, Z.; Lu, X. Application of Raman Spectroscopic Methods in Food Safety: A Review. *Biosensors* **2021**, *11*, 187. [[CrossRef](#)]
98. Quan, Y.; Su, R.; Yang, S.; Chen, L.; Wei, M.; Liu, H.; Yang, J.; Gao, M.; Li, B. In-situ surface-enhanced Raman scattering based on MTi₂₀ nanoflowers: Monitoring and degradation of contaminants. *J. Hazard. Mater.* **2021**, *412*, 125209. [[CrossRef](#)]
99. Wang, L.; Wang, X.; Cheng, L.; Ding, S.; Wang, G.; Choo, J.; Chen, L. SERS-based test strips: Principles, designs and applications. *Biosens. Bioelectron.* **2021**, *189*, 113360. [[CrossRef](#)]
100. Jahn, M.; Patze, S.; Hidi, I.J.; Knipper, R.; Radu, A.I.; Mühlig, A.; Yüksel, S.; Peksa, V.; Weber, K.; Mayerhöfer, T.; et al. Plasmonic nanostructures for surface enhanced spectroscopic methods. *Analyst* **2016**, *141*, 756–793. [[CrossRef](#)]
101. Wang, Z.; Yan, R.; Liao, S.; Miao, Y.; Zhang, B.; Wang, F.; Yang, H. In situ reduced silver nanoparticles embedded molecularly imprinted reusable sensor for selective and sensitive SERS detection of bisphenol A. *Appl. Surf. Sci.* **2018**, *457*, 323–331. [[CrossRef](#)]
102. Xie, J.; Li, L.; Khan, I.M.; Wang, Z.; Ma, X. Flexible paper-based SERS substrate strategy for rapid detection of methyl parathion on the surface of fruit. *Spectrochim. Acta A Mol. Biomol. Spectrosc.* **2020**, *231*, 118104. [[CrossRef](#)]
103. Zhu, C.; Meng, G.; Zheng, P.; Huang, Q.; Li, Z.; Hu, X.; Wang, X.; Huang, Z.; Li, F.; Wu, N. A hierarchically ordered array of silver-nanorod bundles for surface-enhanced Raman scattering detection of phenolic pollutants. *Adv. Mater.* **2016**, *28*, 4871–4876. [[CrossRef](#)] [[PubMed](#)]
104. Li, L.; Lu, Y.; Qian, Z.; Yang, Z.; Yang, K.; Zong, S.; Wang, Z.; Cui, Y. Ultra-sensitive surface enhanced Raman spectroscopy sensor for in-situ monitoring of dopamine release using zipper-like ortho-nanodimers. *Biosens. Bioelectron.* **2021**, *180*, 113100. [[CrossRef](#)] [[PubMed](#)]
105. Juang, R.-S.; Wang, K.-S.; Cheng, Y.-W.; Fu, C.-C.; Chen, W.-T.; Liu, C.-M.; Chien, C.-C.; Jeng, R.-J.; Chen, C.-C.; Liu, T.-Y. Floating SERS substrates of silver nanoparticles-graphene based nanosheets for rapid detection of biomolecules and clinical uremic toxins. *Colloids Surf. A Physicochem. Eng. Asp.* **2019**, *576*, 36–42. [[CrossRef](#)]
106. Li, H.; Wang, Y.; Li, Y.; Qiao, Y.; Liu, L.; Wang, Q.; Che, G. High-sensitive molecularly imprinted sensor with multilayer nanocomposite for 2,6-dichlorophenol detection based on surface-enhanced Raman scattering. *Spectrochim. Acta A Mol. Biomol. Spectrosc.* **2020**, *228*, 117784. [[CrossRef](#)]
107. Wang, Y.; Zhu, G.; Li, M.; Singh, R.; Marques, C.; Min, R.; Kaushik, B.K.; Zhang, B.; Jha, R.; Kumar, S. Water pollutants *p*-cresol detection based on Au-ZnO nanoparticles modified tapered optical fiber. *IEEE Trans. Nanobiosci.* **2021**, *20*, 377–384. [[CrossRef](#)]
108. Usha, S.P.; Gupta, B.D. Urinary *p*-cresol diagnosis using nanocomposite of ZnO/MoS₂ and molecular imprinted polymer on optical fiber based lossy mode resonance sensor. *Biosens. Bioelectron.* **2018**, *101*, 135–145. [[CrossRef](#)]
109. Pathak, A.; Gupta, B.D. Fiber-optic plasmonic sensor utilizing CTAB-functionalized ZnO nanoparticle-decorated carbon nanotubes on silver films for the detection of catechol in wastewater. *ACS Appl. Nano Mater.* **2020**, *3*, 2582–2593. [[CrossRef](#)]